

**Arctic-alpine  
blockfields in  
northern Sweden**

B. W. Goodfellow et al.

This discussion paper is/has been under review for the journal Earth Surface Dynamics (ESurfD).  
Please refer to the corresponding final paper in ESurf if available.

# Arctic-alpine blockfields in northern Sweden: Quaternary not Neogene

**B. W. Goodfellow<sup>1,2</sup>, A. P. Stroeven<sup>1</sup>, D. Fabel<sup>3</sup>, O. Fredin<sup>4,5</sup>, M.-H. Derron<sup>5,6</sup>,  
R. Bintanja<sup>7</sup>, and M. W. Caffee<sup>8</sup>**

<sup>1</sup>Department of Physical Geography and Quaternary Geology, and Bolin Center for Climate Research, Stockholm University, 10691 Stockholm, Sweden

<sup>2</sup>Department of Geology, Lund University, 22362 Lund, Sweden

<sup>3</sup>Department of Geographical and Earth Sciences, East Quadrangle, University Avenue, University of Glasgow, Glasgow G12 8QQ, UK

<sup>4</sup>Department of Geography, Norwegian University of Science and Technology (NTNU), 7491, Trondheim, Norway

<sup>5</sup>Geological Survey of Norway, Leiv Eirikssons vei 39, 7491 Trondheim, Norway

<sup>6</sup>Institute of Geomatics and Risk Analysis, University of Lausanne, 1015 Lausanne, Switzerland

<sup>7</sup>Royal Netherlands Meteorological Institute, Wilhelminalaan 10, 3732 GK De Bilt, the Netherlands

<sup>8</sup>Department of Physics, Purdue University, West Lafayette, Indiana, USA

Title Page

Abstract

Introduction

Conclusions

References

Tables

Figures

◀

▶

◀

▶

Back

Close

Full Screen / Esc

Printer-friendly Version

Interactive Discussion



Received: 22 January 2014 – Accepted: 28 January 2014 – Published: 10 February 2014

Correspondence to: B. W. Goodfellow (brad.goodfellow@natgeo.su.se)

Published by Copernicus Publications on behalf of the European Geosciences Union.

# ESURFD

2, 47–93, 2014

## Arctic-alpine blockfields in northern Sweden

B. W. Goodfellow et al.

Title Page

Abstract

Introduction

Conclusions

References

Tables

Figures



Back

Close

Full Screen / Esc

Printer-friendly Version

Interactive Discussion



## Abstract

Slowly-eroding, blockfield-mantled, non-glacial surface remnants may serve as markers against which to determine Quaternary glacial erosion volumes in high latitude mountain settings. To investigate this potential utility of these surfaces, chemical weathering, erosion rates, and origins of mountain blockfields are investigated in northern Sweden. This is done, firstly, by assessing the intensity of regolith chemical weathering along altitudinal transects descending from three blockfield-mantled summits. Clay/silt ratios, secondary mineral assemblages determined through X-ray diffraction, and the presence of chemically weathered grains visible on scanning electron microscopy, in fine matrix samples collected from pits excavated along the transects are each used for this purpose. Secondly, erosion rates and total surface histories of two of the summits are inferred from concentrations of in situ-produced cosmogenic  $^{10}\text{Be}$  and  $^{26}\text{Al}$  in quartz at the blockfield surface. An interpretative model is adopted that includes temporal variations in nuclide production rates through surface burial by glacial ice and glacial isostasy-induced elevation changes of the blockfield surfaces. Together, our data indicate that these blockfields are not derived from remnants of intensely weathered Neogene weathering profiles, as is commonly considered. Evidence for this interpretation includes minor chemical weathering in each of the three examined blockfields, despite some differences according to slope position. In addition, average erosion rates of  $\sim 16.2 \text{ mm ka}^{-1}$  and  $\sim 6.7 \text{ mm ka}^{-1}$ , calculated for two blockfield-mantled summits, are low but of sufficient magnitude to remove present blockfield mantles, of up to a few meters in thickness, within a late-Quaternary timeframe. Hence, blockfield mantles appear to be replenished by regolith formation through, primarily physical, weathering processes that have operated during the Quaternary. Erosion rates remain low enough, however, for blockfield-mantled, non-glacial surface remnants to provide reasonable landscape markers against which to contrast Quaternary erosion volumes in surrounding glacial landscape elements. The persistence of blockfield mantles over a number of glacial-interglacial cycles and an apparently low likelihood that

ESURFD

2, 47–93, 2014

### Arctic-alpine blockfields in northern Sweden

B. W. Goodfellow et al.

Title Page

Abstract

Introduction

Conclusions

References

Tables

Figures

◀

▶

◀

▶

Back

Close

Full Screen / Esc

Printer-friendly Version

Interactive Discussion



they can re-establish on glacially eroded bedrock, also discounts the operation of a “glacial buzz-saw” on surface remnants that are presently perceived as non-glacial. These interpretations are tempered though by outstanding questions concerning the composition of preceding Neogene regoliths and why they have apparently been comprehensively removed from these remnant non-glacial surfaces. It remains possible that periglacial erosion of perhaps more intensely weathered Neogene regoliths was high during the Pliocene–Pleistocene transition to colder conditions and that periglacial processes reshaped non-glacial surface remnants largely before the formation of block-field armours.

## 1 Introduction

Autochthonous blockfields are diamicts comprised of boulder- to clay-sized regolith formed through in situ bedrock weathering (Potter and Moss, 1968; Nesje et al., 1988; Ballantyne, 1998; Boelhouwers, 2004). They are classically a feature of periglacial landscapes, where they frequently mantle mountain summits and plateaus assumed to have undergone only meters, to tens of meters, of erosion during the Quaternary (Dahl, 1966; Ives, 1966; Sugden, 1968, 1974; Nesje et al., 1988; Rea et al., 1996; Ballantyne, 1998; Small et al., 1999; Goodfellow et al., 2009; Rea, 2013). Blockfield-mantled surfaces may therefore provide useful markers for quantifying Quaternary glacial erosion volumes (Nesje and Whillans, 1994; Glasser and Hall, 1997; Kleman and Stroeven, 1997; Staiger et al., 2005; Goodfellow, 2007; Jansson et al., 2011). However, recent studies of landscape evolution and Quaternary sediment budgets along the Norwegian margin (Nielsen et al., 2009; Steer et al., 2012), imply that, rather than providing these markers, autochthonous blockfield-mantled surfaces have also undergone surface lowering of some hundreds of meters through the action of a Quaternary glacial and periglacial “buzz-saw”. Hence, because the origins, ages, and erosion rates of blockfields remain enigmatic, their utility for estimating Quaternary erosion volumes is still contentious. In this study we therefore address the weathering characteristics,

## Arctic-alpine blockfields in northern Sweden

B. W. Goodfellow et al.

Title Page

Abstract

Introduction

Conclusions

References

Tables

Figures



Back

Close

Full Screen / Esc

Printer-friendly Version

Interactive Discussion



erosion rates, and formation ages of autochthonous blockfields in the periglaci-ated northern Swedish mountains.

Autochthonous blockfields in periglaci-ated landscapes have been frequently consid-ered to represent remnants of Neogene weathering profiles (Caine, 1968; Ives, 1974; Clapperton, 1975; Nesje et al., 1988; Rea et al., 1996; Boelhouwers et al., 2002; André, 2003; Marquette et al., 2004; Sumner and Meiklejohn, 2004; Fjellanger et al., 2006; Paasche et al., 2006; André et al., 2008; Strømsøe and Paasche, 2011). According to this model, block production was initiated through chemical weathering of bedrock under a warmer-than-present climate during the Neogene. Regolith stripping occurred during the colder Quaternary, subaerially exposing rock made more porous by chemical weathering. Enhanced access by water permitted subsequent efficient frost shattering of this rock, which was periglacially reworked to produce blockfield mantles that armour surfaces and are resistant to further modification (Boelhouwers, 2004).

By making the critical assumption that chemical weathering depends upon a “warm” climate, certain characteristics of blockfields have been argued to be incompatible with a Quaternary origin. These characteristics include the presence of saprolite (Caine, 1968) and/or secondary minerals, especially kaolinite and gibbsite (Rea et al., 1996; Fjellanger et al., 2006; André et al., 2008; Strømsøe and Paasche, 2011), and clay abundances exceeding about 10% of the fine matrix (clay, silt, sand) volume (Rea et al., 1996; Strømsøe and Paasche, 2011). Additionally, there are apparently no actively forming blockfields (Boelhouwers, 2004), with the exception of those developing on highly frost susceptible limestone in the Canadian Arctic (Dredge, 1992). Together with the occurrence of blockfields on surface remnants that do not appear to have been glacially eroded (Sugden, 1968, 1974; Kleman and Stroeven, 1997; Stroeven et al., 2002; Fabel et al., 2002; Marquette et al., 2004; Goodfellow, 2007), this obser- vation provides further evidence that blockfields may have residence times exceeding the last glacial-interglacial cycle. By considering these field observations together with the geochemical features, regolith residence times have been argued to extend back

## ESURFD

2, 47–93, 2014

### Arctic-alpine blockfields in northern Sweden

B. W. Goodfellow et al.

Title Page

Abstract

Introduction

Conclusions

References

Tables

Figures

◀

▶

◀

▶

Back

Close

Full Screen / Esc

Printer-friendly Version

Interactive Discussion



to the Neogene (Rea et al., 1996; Whalley et al., 2004; André et al., 2008; Strømsøe and Paasche, 2011).

Although the Neogene-origin model is usually invoked, some workers conclude that blockfields in periglaciated landscapes have entirely Quaternary origins (Dahl, 1966; Dredge, 1992; Ballantyne, 1998, 2010; Ballantyne et al., 1998; Goodfellow et al., 2009; Goodfellow, 2012). According to the Quaternary-origin model, blockfields are produced through synergistic physical- (e.g. frost) and chemical weathering processes (Whalley et al., 2004), which operate independently of preconditioning by Neogene processes.

Key evidence supporting the Quaternary-origin model includes comparatively slow formation of clay-sized regolith and secondary minerals through chemical weathering. This is indicated, firstly, by a low ratio of clay to silt across a sample batch (clay <math>\sim 0.5 \cdot \text{silt}</math>), compared with higher ratios (clay >math>\sim 0.5 \cdot \text{silt}</math>) in regoliths located in non-periglaciated settings (Goodfellow, 2012). Secondly, low abundances of secondary minerals are mixed in with abundant primary minerals (Goodfellow, 2012). The secondary mineral assemblages may span a range of leaching intensities from low (minerals with interstratified primary and secondary layers), across moderate (2 : 1 layer minerals such as vermiculite) and high (1 : 1 minerals such as kaolinite), to extreme (Al- and Fe-oxides). This may reflect the effect of heterogeneity in regolith hydrology on weathering intensity in blockfields and the varying susceptibility of different primary minerals to chemical weathering. These assemblages differ from those occurring in sub-tropical and tropical regoliths, which are generally simpler and dominated by high volumes (i.e. > 30 % of the regolith) of kaolinite and Al- and Fe-oxides (Meunier et al., 2007; White et al., 1998; Goodfellow, 2012).

In the Quaternary-origin model it is further argued that blocks form by frost weathering *within* the regolith, near the base of the permafrost active layer where liquid water accumulates and seasonally refreezes (Dahl, 1966; Anderson, 1998; Small et al., 1999; Goodfellow et al., 2009; Ballantyne, 2010). This mechanism might therefore explain the apparent absence of frost weathering of clasts comprising blockfield surfaces, while fur-

## ESURFD

2, 47–93, 2014

### Arctic-alpine blockfields in northern Sweden

B. W. Goodfellow et al.

Title Page

Abstract

Introduction

Conclusions

References

Tables

Figures

◀

▶

◀

▶

Back

Close

Full Screen / Esc

Printer-friendly Version

Interactive Discussion



ther highlighting a possible key role of Quaternary, rather than Neogene, weathering processes in blockfield formation.

A key problem with ascertaining blockfield ages and origins is that it has, until recently, been impossible to measure blockfield erosion rates or subaerial exposure durations. However, measurements of terrestrial cosmogenic nuclide (TCN) concentrations now offer some insight into these issues. Erosion rates of 1.1–12 mmka<sup>-1</sup> have been measured for subaerially exposed bedrock within blockfields (Small et al., 1997; Bierman et al., 1999; Phillips et al., 2006). These rates may be lower than in the surrounding blockfields, because exposed bedrock sheds, rather than retains, water (Small et al., 1999; Cockburn and Summerfield, 2004; Phillips et al., 2006). However, regolith erosion rates in summit blockfields may remain low because of armouring of gently sloping surfaces by cobbles and boulders (Granger et al., 2001). For example, erosion rates of 13.4–14 mmka<sup>-1</sup> have been measured in plateau blockfields in the Wind River Range, Wyoming, which have not been inundated by glacial ice (Small et al., 1999). Where non-erosive cold-based ice has buried blockfields during glacial periods (Sugden and Watts, 1977; Kleman and Stroeven, 1997; Bierman et al., 1999; Hättestrand and Stroeven, 2002; Briner et al., 2003; Marquette et al., 2004), time-averaged erosion rates are further lowered. Subaerial exposure and burial durations of blockfield regoliths might then extend back to the early Quaternary or late Neogene. By combining measurements of TCN concentrations in bedrock or regolith with an inferred history of surface burial by ice sheets from benthic  $\delta^{18}\text{O}$  records (Fabel et al., 2002; Stroeven et al., 2002; Li et al., 2008), it is possible to estimate minimum time spans over which present blockfield regoliths have mantled surfaces.

The aim of this study is to test whether blockfields in the northern Swedish mountains are remnants of intensely-weathered Neogene regoliths or are formed solely by Quaternary weathering processes. Firstly, we test the intensity of chemical weathering through grain size, X-ray diffraction (XRD), and scanning electron microscopy (SEM) analyses of blockfield fine matrix along three hillslope transects. Secondly, we examine total surface histories of two summit blockfields through the combination of apparent

## Arctic-alpine blockfields in northern Sweden

B. W. Goodfellow et al.

Title Page

Abstract

Introduction

Conclusions

References

Tables

Figures



Back

Close

Full Screen / Esc

Printer-friendly Version

Interactive Discussion



## Arctic-alpine blockfields in northern Sweden

B. W. Goodfellow et al.

Title Page

Abstract

Introduction

Conclusions

References

Tables

Figures

◀

▶

◀

▶

Back

Close

Full Screen / Esc

Printer-friendly Version

Interactive Discussion



surface exposure durations, measured through TCN analyses, with burial periods, determined through an ice sheet model driven by benthic  $\delta^{18}\text{O}$  records. Incorporating an elastic lithosphere, relaxed asthenosphere (ELRA) bedrock model, the ice sheet model is also used to study the effects of bedrock isostatic response to glacial loading and unloading on nuclide production rates (which vary with elevation above sea level) and subsequent total surface histories. Because uncertainties associated with calculations of the total surface history are large, we confine our enquiry to an order of magnitude question: are total surface histories likely confined to the late Quaternary ( $< 1$  Ma) or do they extend to the early Quaternary/late Neogene? A Neogene origin would imply low Quaternary-averaged surface erosion rates and a utility of autochthonous blockfield-mantled surfaces as markers from which to estimate glacial erosion of surrounding glacial landscapes. In contrast, the implications of a Quaternary origin are more ambiguous. These could not exclude tens of meters, to perhaps more than one hundred meters, of surface lowering during the Plio–Pleistocene transition of currently blockfield-mantled surfaces, resulting in a lowered utility of these surfaces as markers from which to estimate glacial erosion of surrounding glacial landscapes.

## 2 Study area

Blockfields were examined along hillslope transects descending from three summits in the northern Swedish mountains (Fig. 1); Alddasçorru ( $68^{\circ}25' \text{ N}$ ,  $19^{\circ}24' \text{ E}$ ; 1538 m above sea-level [a.s.l.]), Duopteçohkka ( $68^{\circ}24' \text{ N}$ ,  $19^{\circ}22' \text{ E}$ ; 1336 m a.s.l.), and Tarfatljårro ( $67^{\circ}55' \text{ N}$ ,  $18^{\circ}39' \text{ E}$ ; 1626 m a.s.l.). The transects intersect slope units shaped by contrasting assemblages of surface processes. Regolith diffusion has shaped gently convex summits, whereas solifluction has operated on higher gradient down-slope segments. On the steepest, lower-most slopes imbricated blocks and boulder sheets indicate that shallow landsliding and boulder tumbling have been active in addition to solifluction. Further deposition of transported material has occurred at the concave bases of these slopes where scattered boulders are embedded in, and rest



## Arctic-alpine blockfields in northern Sweden

B. W. Goodfellow et al.

Title Page

Abstract

Introduction

Conclusions

References

Tables

Figures

◀

▶

◀

▶

Back

Close

Full Screen / Esc

Printer-friendly Version

Interactive Discussion



the ground of  $-4.3^{\circ}\text{C}$  and mean annual ground temperatures of  $-2.8^{\circ}\text{C}$  and  $-3.0^{\circ}\text{C}$ , at 0.2 m depth and 2.5 m depth respectively, over 2003–2005 (Isaksen et al., 2007). The closest meteorological station to Alddasčorru and Duoptečohkka is located at the Abisko Scientific Research Station at 380 m a.s.l. (Fig. 1), which has a warmer and drier climate than occurs on Tarfalatjårro, with a MAAT of  $-0.9^{\circ}\text{C}$  and MAP of about 320 mm (Eriksson, 1982). Based on this MAAT and an adiabatic lapse rate of  $-0.6^{\circ}\text{C}$  per 100 m, MAATs of  $-8.1^{\circ}\text{C}$  and  $-6.9^{\circ}\text{C}$  are estimated for Alddasčorru and Duoptečohkka, respectively. Permafrost is present on each of the three summits, with the monitoring borehole on Tarfalatjårro indicating a distinct warming trend and a present active layer thickness of 1.4–1.6 m (Isaksen et al., 2001, 2007). Snow covers Tarfalatjårro from about October to May, although strong winds limit the maximum snow depth to about 0.3 m (Isaksen et al., 2001). Similar snow and permafrost conditions are expected and assumed for Alddasčorru and Duoptečohkka. Vegetation along each transect is restricted to lichens, mosses, and occasional grasses, except for the base of the Duoptečohkka transect, which is well grassed. Stable lichen-covered surface clasts indicate that, although they have occurred in the past, large-scale periglacial sorting and gelifluction processes appear to be now largely inactive. However, upfreezing of pebbles and creep and gelifluction processes over a few tens of centimetres remain active.

The northern Swedish mountains have been repeatedly glaciated during the Quaternary, with cirque glaciation inferred to have been dominant before 2.0 million years ago (Ma), mountain ice sheets dominant between 2.0 and 0.7 Ma, and Fennoscandian ice sheets developing over the last 0.7 Ma (Kleman and Stroeven, 1997; Kleman et al., 2008). Current glaciation in the region is confined to small cirque and valley glaciers. During glacial periods, relatively high altitude surfaces such as Tarfalatjårro, Alddasčorru, and Duoptečohkka have been either nunataks or were covered by cold-based ice sheets (Stroeven et al., 2006). The occasional erratics on Tarfalatjårro and abundant granitic erratics on Alddasčorru and the flanks of Duoptečohkka confirm former ice sheet coverage as late as 12 ka (Fabel et al., 2002; Stroeven et al., 2006).



0.60 m depth samples were processed. For comparative purposes, fine matrix samples were taken for grain size, XRD, and SEM analyses from summit till covers on Ruohthakörru (Fig. 1; 68°09' N, 19°20' E; 1342–1346 m a.s.l.; 3 samples from 0.5, 0.9, and 1.2 m depth) and on Nulpotjåkka (Fig. 1; 67°48' N, 18°01' E; 1405 m a.s.l.; 1 sample from 0.9 m depth).

The Tarfalatjärro summit pit was excavated where a shattered quartz vein (~ 8 m in length) was visible on the blockfield surface. A clast of vein quartz (3–4 cm thick) was collected to determine apparent surface exposure durations from in situ-produced  $^{10}\text{Be}$  and  $^{26}\text{Al}$  concentrations. Because the quartz vein was clearly expressed at the blockfield surface, and because periglacially sorted circles were widely dispersed and weakly defined, zero vertical mixing of the sampled clast through the regolith profile was assumed.

Similarly, a surface clast (4 cm thick) of vein quartz was sampled from the summit of Duoptečohkka, also for measurement of in situ-produced  $^{10}\text{Be}$  and  $^{26}\text{Al}$  concentrations. Zero vertical mixing of the sampled clast through the regolith was again assumed because this long clast (0.19 m) resided on the surface of a thin regolith (0.30 m depth). Furthermore, periglacially sorted circles were absent from this site. Because of the absence of glacial erratics from this summit and the presence of quartz veins in these blockfields, we considered the sampled clast to be locally derived. Sampling of vein quartz clasts was undertaken on a summit crest, both here and on Tarfalatjärro, to eliminate the possibility of these clasts having been transported and buried by slope processes, which would complicate estimates of total surface histories from measurements of  $^{10}\text{Be}$  and  $^{26}\text{Al}$  concentrations. This constraint coupled with the scarcity of summit vein quartz limited our sampling for TCN analyses to these two sites.

To correct for topographic shielding the surface geometries of the sampled blockfields and surrounding summits were measured with a clinometer and compass. Sample locations were recorded with a handheld GPS and on a 1 : 50 000 topographic map. Three amphibolite clasts and three fine matrix samples extracted in a cylinder of known volume were collected for regolith clast and matrix density measurements.

## Arctic-alpine blockfields in northern Sweden

B. W. Goodfellow et al.

Title Page

Abstract

Introduction

Conclusions

References

Tables

Figures

◀

▶

◀

▶

Back

Close

Full Screen / Esc

Printer-friendly Version

Interactive Discussion



## 3.2 Fine matrix analyses

To determine the weathering characteristics of blockfields, grain size, SEM, and XRD analyses were completed at the Geological Survey of Norway, Trondheim. Grain sizes were determined on dried samples with a Coulter LS Particle Size Analyser. SEM analyses were performed on surface bulk fine matrix samples and semi-quantitative analyses of grain chemistry and mineralogy were completed according to energy dispersive spectrometer techniques (Goldstein et al., 2003). Thin sections for mineralogical interpretation of parent material were prepared from two Alddasçorru rock samples.

For XRD analysis, the  $< 2 \mu\text{m}$  size fraction of each sample was separated by settling, Mg-saturated, and purified with a ceramic filter to produce oriented samples. An initial XRD scan was performed at  $2-69^\circ 2\theta$  with a scan speed of  $0.02^\circ 2\theta \text{ s}^{-1}$  and a step size of  $0.04^\circ 2\theta$ . Second and third scans were performed following ethylglycol saturation and heating of the samples to  $550^\circ\text{C}$ , respectively. These scans were performed at  $2-35^\circ 2\theta$  with a scan speed of  $0.0067^\circ 2\theta \text{ s}^{-1}$  and a step size of  $0.04^\circ 2\theta$ . Diffraction peaks were analysed with peak search software and manually reviewed using Brindley and Brown (1980) and Moore and Reynolds (1997).

## 3.3 Cosmogenic radionuclide analyses and ice sheet modelling

Concentrations of  $^{10}\text{Be}$  and  $^{26}\text{Al}$  in samples of vein quartz were measured to estimate erosion rates and residence times of blockfields. Clean quartz separates were processed for cosmogenic nuclide analyses through methods adapted from Kohl and Nishiizumi (1992) and Child et al. (2000). Accelerator mass spectrometry (AMS) measurement of the Tarfalatjårro sample was completed at PRIME Lab, Purdue University, USA, and AMS measurement of the Duopteçohkka sample was completed at the SUERC AMS Laboratory, East Kilbride, UK. Measured TCN concentrations were corrected by full chemistry procedural blanks and normalized using the NIST  $^{10}\text{Be}$  standard (SRM4325) with a  $^{10}\text{Be}/^9\text{Be}$  ratio of  $(2.79 \pm 0.03) \times 10^{-11}$  and using a  $^{10}\text{Be}$  half-life of  $1.36 \times 10^6$  a (Nishiizumi et al., 2007) and the PRIME Lab  $^{26}\text{Al}$  standard (Z92-0222)

ESURFD

2, 47–93, 2014

### Arctic-alpine blockfields in northern Sweden

B. W. Goodfellow et al.

Title Page

Abstract

Introduction

Conclusions

References

Tables

Figures

◀

▶

◀

▶

Back

Close

Full Screen / Esc

Printer-friendly Version

Interactive Discussion



with a nominal  $^{26}\text{Al}/^{27}\text{Al}$  ratio of  $4.11 \times 10^{-11}$  and using an  $^{26}\text{Al}$  half-life of  $7.05 \times 10^5$  a (Nishiizumi, 2004). Errors in nuclide concentrations include the quadrature sum of analytical uncertainty calculated from AMS counting statistics and procedural errors.

Apparent exposure ages were calculated from  $^{10}\text{Be}$  and  $^{26}\text{Al}$  concentrations using the CRONUS-Earth Exposure age calculator (version 2.2; Balco et al., 2008) assuming zero erosion and the Lal/Stone time-independent  $^{10}\text{Be}$  production rate model (Lal, 1991; Stone, 2000). The time-independent Lal/Stone scaling was used here because we also used it for modelling total surface histories for reasons described below. We do though cite in our results the full age ranges given for all production rate models incorporated into the CRONUS-Earth Exposure age calculator. Corrections were applied for topographic shielding (scaling factors  $> 0.9998$ ) and for sample thickness using a clast density of  $2.65 \text{ g cm}^{-3}$ . No corrections were applied for snow or vegetation shielding. Quoted exposure age uncertainties ( $1\sigma$  external) include nuclide production rate uncertainties and the concentration errors described above.

Total surface histories, incorporating periods of subaerial exposure and burial by ice sheets, of the Duoptečohkka and Tarfalatjårro summit blockfields were calculated from measured  $^{10}\text{Be}$  concentrations according to the following equation (rearranged from Lal, 1991):

$$\frac{N_i}{N} = [1 - \beta] \exp\{(\lambda + \alpha)t\} + \beta \quad (1)$$

where  $N$  = nuclide concentration, with the subscript  $i$  indicating one step back in time;  $\lambda$  = nuclide half-life;  $t$  = time step, and;

$$\alpha = \frac{E\rho}{\Lambda} \quad (2)$$

**Arctic-alpine  
blockfields in  
northern Sweden**

B. W. Goodfellow et al.

Title Page

Abstract

Introduction

Conclusions

References

Tables

Figures

◀

▶

◀

▶

Back

Close

Full Screen / Esc

Printer-friendly Version

Interactive Discussion



where  $E$  = erosion rate ( $\text{cm a}^{-1}$ );  $\rho$  = regolith density, and;  $\Lambda$  = attenuation mean free path, and;

$$\beta = \frac{P}{N(\lambda + \alpha)} \quad (3)$$

5 where  $P$  = nuclide production rate. During periods of surface burial by ice sheets, equation (1) is simplified to:

$$\frac{N_i}{N} = \exp\{\lambda t\} \quad (4)$$

Total surface histories are obtained when zero nuclide concentrations are reached.

10 The source code for the CRONUS-Earth exposure age calculator (version 2.2; Balco et al., 2008) was not used for calculating these total surface histories because of the complexities introduced by accounting for depth- and time-averaged  $^{10}\text{Be}$  production rates. Rather, a sea-level high latitude ( $> 60^\circ$ )  $^{10}\text{Be}$  production rate of  $4.59 \pm 0.28 \text{ atoms g}^{-1} \text{ a}^{-1}$ , from the Nishiizumi et al. (2007)  $^{10}\text{Be}$  half-life of  $1.36 \times 10^6$   
15 a, was used in these calculations. Production rates were scaled to latitude and altitude using Stone (2000) and a sea surface temperature of  $5^\circ\text{C}$ . The errors in total surface histories attributable to our use of simplified  $^{10}\text{Be}$  production rates are minor compared with uncertainties attributable to surface burial by snow and ice and isostatic responses to ice sheet loading and unloading. A constant blockfield density of  $2.60 \text{ g cm}^{-3}$  was assumed based on a blockfield containing 15 % fine matrix, with a density of  $2.10 \text{ g cm}^{-3}$   
20 (mean of 3 samples,  $1\sigma = 0.09$ ), and 85 % amphibolite, with a density of  $2.79 \text{ g cm}^{-3}$  (mean of 3 samples,  $1\sigma = 0.02$ ). The effects of regolith dissolution were ignored because total surface histories that include multiple periods of surface exposure and burial by ice sheets preclude erosion rate calculations directly from nuclide concentrations.  
25 Furthermore, chemical weathering in these blockfields was likely to be minor (Goodfellow et al., 2009). Corrections were applied for shielding and for sample thickness using an attenuation mean free path of  $160 \text{ g cm}^{-2}$  and a quartzite density of  $2.65 \text{ g cm}^{-3}$ .

## Arctic-alpine blockfields in northern Sweden

B. W. Goodfellow et al.

Title Page

Abstract

Introduction

Conclusions

References

Tables

Figures



Back

Close

Full Screen / Esc

Printer-friendly Version

Interactive Discussion



**Arctic-alpine  
blockfields in  
northern Sweden**

B. W. Goodfellow et al.

Title Page

Abstract

Introduction

Conclusions

References

Tables

Figures

◀

▶

◀

▶

Back

Close

Full Screen / Esc

Printer-friendly Version

Interactive Discussion



A correction for snow burial was also incorporated assuming 0.3 m of snow (Isaksen et al., 2007), with a density of  $0.3 \text{ g cm}^{-3}$ , for a duration of seven months per year. The resulting annual shielding by snow of only  $5.25 \text{ g cm}^{-2}$  is assumed to be representative of all ice free periods. Associated uncertainties are, however, unknown but, because they are potentially high, a sensitivity analysis was performed by increasing the depth of burial from 0.30 m to 0.50 m and increasing duration of burial from seven to ten months a year in a total surface history calculation.

To incorporate periods of surface burial by ice sheets into total surface history calculations, and to explore the effects of glacial isostasy on these calculations, we used a 3-dimensional ice-dynamical model forced by the Lisiecki and Raymo (2005) stack of global benthic  $\delta^{18}\text{O}$  records and an ELRA bedrock model. Full details of the ice-dynamical model can be found in Bintanja et al. (2002, 2005). An ELRA model offers the best glacial isostasy approximation among the group of simple models, with its primary weakness being that it incorporates only one time constant (Le Meur and Huybrechts, 1996). Whereas self-gravitating visco-elastic spherical Earth models are the most accurate, they are much more complex and require greater computational power and time (Le Meur and Huybrechts, 1996). The ice sheet model was run at 40 km resolution, with a 100 yr time step over the last 1.07 Ma. Although spatial resolution is coarse, using a 20 km grid provides minimal change in bedrock topography and calculations on a 50 m Digital Elevation Model of the northern Swedish mountains produced the same mean elevations for  $40 \times 40 \text{ km}$  squares centred on the relevant model grid points. Furthermore, the wavelength of glacial isostasy is much longer than the topographic wavelength (Le Meur and Huybrechts, 1996). Regional ice sheet thickness is subsequently more important than local ice sheet thicknesses for determining isostatic response and a grid size of some tens of kilometres appears justified. We therefore consider our model to offer a reasonable approximation (with estimated  $\pm 20\%$  error margins) of both ice sheet burial durations and of glacial isostasy.

## 4 Results

### 4.1 Blockfield structure

Blockfield vertical sections along the Alddasčorru, Duoptečohkka, and Tarfalatjårro altitudinal transects display a number of common features (Fig. 2). Extensive lichen covers and rounding of subaerially exposed clast surfaces through granular disintegration indicate present ground surface stability. Where the coarse parts of periglacially sorted circles and stripes intersect, a surface layer of cobbles and boulders is underlain by a layer of gravel and cobbles to average depths of 0.9–1.0 m. Where fine matrix-rich sorted circle centres intersect, a surface layer of cobbles and boulders is usually underlain by fine matrix, granules and gravel, in which cobbles or boulders are embedded, to depths up to 0.7 m. Pits were excavated until large amphibolite slabs prohibited sampling of deeper sections (pit depths ranged between 0.63 and 1.30 m). The Duoptečohkka summit pit was an exception, because bedrock occurred at only 0.30 m. The bottom of each pit typically consisted of boulders embedded in a fine matrix that ranged from damp to water saturated (Table A.1). None of the pits revealed soil horizons or saprolite.

Although only about 10% of the ground surface consists of fine matrix, it appears to comprise about 10–20% of the subsurface regolith (Table A.1). Surface fine matrix is most abundant on the section of the plateau into which Alddasčorru pit 4 was dug (~50% of the surface area) and in the saddle into which Tarfalatjårro pits 6–9 were dug (~30% of the surface area). Sub-surface fine matrix appears most limited on the summits of Alddasčorru and Tarfalatjårro (5–15%), and in the solifluction lobes on the slope of Duoptečohkka (pits 4 and 5, 5–10%; Table A.1). Here, cobbles and boulders were embedded by gravel throughout most of the subsurface, with only small accumulations of fine matrix on boulder tops or in poorly-defined sorted circle centres.

In summary, blockfield sections indicate present surface stability, but also regolith sorting and transport during former periods of colder climate where blockfield-mantled

ESURFD

2, 47–93, 2014

### Arctic-alpine blockfields in northern Sweden

B. W. Goodfellow et al.

Title Page

Abstract

Introduction

Conclusions

References

Tables

Figures

◀

▶

◀

▶

Back

Close

Full Screen / Esc

Printer-friendly Version

Interactive Discussion



surfaces remained free of glacial ice cover. Chemical weathering rates have been insufficient to produce soil horizons or saprolite.

## 4.2 Fine matrix granulometry

All blockfield fine matrix samples are sandy loams (Table 1; US Department of Agriculture, 1993, p. 138). However, minor variations remain in the distribution of sand ( $1\sigma = 7.5\%$ ), silt ( $1\sigma = 6.9\%$ ), and clay ( $1\sigma = 1.3\%$ ) according to sampling depth and the subsurface distribution of boulders, between which coarser matrix accumulates. Till samples vary between loamy sand, sandy loam, and silt loam, and have lower mean clay quantities ( $1.8\%$ ,  $1\sigma = 1.1\%$ ) than the blockfield fine matrix ( $4.2\%$ ,  $1\sigma = 1.3\%$ ).

Although the clay contents of blockfields are higher than of till, it comprises only  $1.5\%$  to  $5.8\%$  of the fine matrix volume, which remains at the low end of the range ( $1\text{--}30\%$ ) previously reported for other blockfields (e.g., Caine, 1968; Rea et al., 1996; Dredge, 2000; Marquette et al., 2004; Paasche et al., 2006; Table A.1 in Goodfellow, 2012). Clay-silt ratios are all  $\leq 0.14$  (Table 1; Fig. 3). These indicate a low intensity of chemical weathering that is typical for regolith formation under, at least seasonal, periglacial conditions (Goodfellow, 2012).

## 4.3 Fine matrix mineralogy

XRD analyses of the clay-sized fraction of the regolith indicate the presence of primary and secondary minerals in all samples (Table 1, Fig. 4). Primary minerals are abundant and include chlorite, amphibole, and feldspar. The presence of these minerals, along with epidote, was also confirmed using thin sections. In addition to these primary minerals, small quantities of poorly crystallized Al- and Fe-oxyhydroxides are identifiable by XRD in the Alddasčorru and Tarfalatjårro summit samples. In contrast, vermiculite, gibbsite, and larger quantities of poorly crystallized oxyhydroxides are also identifiable in concave locations, such as at the base of Alddasčorru and in the Tarfalatjårro saddle. Gibbsite generally occurs together with both poorly crystallized Al-

### Arctic-alpine blockfields in northern Sweden

B. W. Goodfellow et al.

Title Page

Abstract

Introduction

Conclusions

References

Tables

Figures

◀

▶

◀

▶

Back

Close

Full Screen / Esc

Printer-friendly Version

Interactive Discussion



and Fe-oxyhydroxides and vermiculite. A sample from the upper slope of Alddasčorru (BG-05-26; Fig. 4b) forms a possible exception, where poorly crystallized oxyhydroxides and gibbsite, only, appear to be present. All till samples contain poorly crystallized oxyhydroxides and vermiculite, but only one or, perhaps, two samples of mixed colluvium and till at the base of the Duoptečohkka transect also contain gibbsite. There is no variation in secondary mineral assemblages either with location across periglacially sorted circles or with depth beneath the ground surface (Goodfellow et al., 2009). However, there is some intra-site variation in the presence of gibbsite along lower slopes of the Duoptečohkka transect. We were unable to distinguish kaolinite according to the standard XRD techniques we used because of the ubiquitous presence of chlorite (Moore and Reynolds, 1997, p. 234). However, we consider that kaolinite may be present in our samples in small quantities. Quartz and muscovite are also commonly present. Because of the amphibolite parent rock and scarcity of quartz veins these likely represent aeolian additions to blockfields and/or are till components.

SEM scans reveal an almost ubiquitous absence of chemical weathering, even on easily weathered minerals such as albite, amphibole, and epidote. That chemical weathering was established for two albite grains, one through surface etching and a second through more general disintegration (Fig. 5), strengthens the importance of the lack of chemical weathering in other samples.

In summary, XRD and SEM analyses indicate chemical weathering in all blockfield and till samples, albeit in limited quantities. Samples from concave blockfield sites appear most chemically weathered and summit blockfield fine matrix appears the least chemically weathered. Chemical weathering of till samples displays an intermediate intensity.

#### 4.4 Total surface histories

Apparent  $^{10}\text{Be}$  surface exposure durations for two surface quartzite clasts on Duoptečohkka and Tarfalatjärro are  $33.5 \pm 3.2$  ka and  $81.8 \pm 7.8$  ka, respectively (Table 2). These ages are based on the time-invariant spallogenic production rate model

**Arctic-alpine  
blockfields in  
northern Sweden**

B. W. Goodfellow et al.

Title Page

Abstract

Introduction

Conclusions

References

Tables

Figures



Back

Close

Full Screen / Esc

Printer-friendly Version

Interactive Discussion



(Lal, 1991; Stone, 2000; Balco et al., 2008). For Duoptečohkka, this provides a younger age than any of the time-varying  $^{10}\text{Be}$  spallogenic production rate models included on the CRONUS-Earth exposure age calculator (version 2.2; Balco et al., 2008). The full apparent surface exposure age range is  $33.5 \pm 3.2$  ka to  $35.6 \pm 4.4$  ka. For Tarfalatjårro, the apparent surface exposure age range from these production rate models is  $80.4 \pm 8.5$  ka to  $86.2 \pm 10.8$  ka.

The  $^{26}\text{Al}/^{10}\text{Be}$  ratio of  $6.57 \pm 0.43$  for the quartz sample of the Duoptečohkka summit (Table 2) indicates no apparent burial (within error) by the Fennoscandian Ice Sheet. However, even a full exposure nuclide ratio does not exclude a complex exposure history including short intermittent periods of surface burial beneath an ice sheet. In contrast, the lower ratio of  $5.92 \pm 0.41$  for the quartz sample of the Tarfalatjårro surface requires some previous period of burial, and, by inference, indicates periods of burial by glacial ice.

Model results for ice sheet surface elevations, ice sheet thicknesses, and glacial isostasy over multiple glacial cycles indicate that the Duoptečohkka and Tarfalatjårro summits have been repeatedly covered by ice sheets (Fig. 6). According to the model, thicker ice has formed over Duoptečohkka (a maximum of 1595 m compared with 1150 m for Tarfalatjårro) and burial durations have been longer on this summit. These data are consistent with what might be expected for the lower elevation of Duoptečohkka (1336 m a.s.l. vs. 1626 m a.s.l. for Tarfalatjårro). However, they seemingly contrast with inferences from the  $^{26}\text{Al}/^{10}\text{Be}$  ratio for Duoptečohkka (Table 2) of either no glacial burial of this summit or surface burial during short periods relative to intermittent full-exposure durations. The thickness and duration of ice cover may therefore be over-estimated in our model and a comparison with data from other models supports this possibility. Firstly, ice sheet thicknesses produced by our model are either similar to those indicated for our study areas by other ice sheet models (Fjeldskaar et al., 2000; Milne et al., 2004; Peltier, 2004; Steffen and Kauffman, 2005) or exceed them (Peltier, 1994; Kauffman et al., 2000; Lambeck et al., 2006; Steffen et al., 2006; Charbit et al., 2007). Secondly, the magnitude of isostatic rebound following the last

**Arctic-alpine  
blockfields in  
northern Sweden**

B. W. Goodfellow et al.

Title Page

Abstract

Introduction

Conclusions

References

Tables

Figures

◀

▶

◀

▶

Back

Close

Full Screen / Esc

Printer-friendly Version

Interactive Discussion



glaciation is 497 m for Duoptečohkka and 457 m for Tarfalatjårro. These values exceed those indicated by the isostatic rebound map in the National Atlas of Sweden (Fredén, 2002, p. 101) by 150–250 m, which again indicates a possible over-estimation of ice sheet thicknesses and durations of ice coverage by our model. The key consequences of this for our subsequent analysis of total surface histories are that the time available for cosmogenic nuclide accumulation and the rate at which they accumulate are likely underestimated, whereas decay periods during ice sheet burial are likely over-estimated. Because nuclides have likely accumulated in surface regolith at a faster rate than provided for in our model and nuclide decay has likely been less, inferred maximum erosion rates will be underestimated and total surface histories, for a given erosion rate, will be overestimated. We consider the total surface history calculations to remain valid for our purposes, however, because we are interested in an order of magnitude question (i.e., whether or not total surface histories are confined to the late Quaternary) and to be conservative in our interpretations prefer to err on the side of over-estimating total surface histories.

Modelled total surface histories for Duoptečohkka and Tarfalatjårro are shown in Fig. 7. Steps in these total surface history curves indicate periods of intermittent surface burial by glacial ice. Where these steps occur in each modelled scenario varies according to erosion rate and duration of surface burial by glacial ice. The primary model output, which considers the effects of both ice sheet burial and bedrock isostasy on cosmogenic nuclide accumulation (labelled “burial and isostasy”), indicates a maximum surface erosion rate of  $\sim 16.2 \text{ mm ka}^{-1}$  for Duoptečohkka and  $\sim 6.7 \text{ mm ka}^{-1}$  for Tarfalatjårro. At maximum surface erosion rates, maximum surface ages become infinite. However, the total surface histories of Duoptečohkka and Tarfalatjårro become asymptotic above cut-off values of  $\sim 290 \text{ ka}$  and  $\sim 390 \text{ ka}$  before present, respectively. This offers suggestive evidence that the late Quaternary has likely offered sufficient time for the present regolith mantles on both summits to gain their respective  $^{10}\text{Be}$  inventories.

**Arctic-alpine  
blockfields in  
northern Sweden**

B. W. Goodfellow et al.

Title Page

Abstract

Introduction

Conclusions

References

Tables

Figures

◀

▶

◀

▶

Back

Close

Full Screen / Esc

Printer-friendly Version

Interactive Discussion



## Arctic-alpine blockfields in northern Sweden

B. W. Goodfellow et al.

Title Page

Abstract

Introduction

Conclusions

References

Tables

Figures

◀

▶

◀

▶

Back

Close

Full Screen / Esc

Printer-friendly Version

Interactive Discussion



Four additional total surface history scenarios help define the sensitivity of derived maximum erosion rates to durations of surface burial by snow and glacial ice and to the magnitude of glacial isostasy (Fig. 7). As expected, maximum erosion rates are highest in the absence of former glaciation (“0 burial, 0 isostasy” lines in Fig. 7). These rates are  $\sim 18.2 \text{ mm ka}^{-1}$  for Duoptečohkka and  $\sim 7.3 \text{ mm ka}^{-1}$  for Tarfalatjårro. Accordingly, total surface histories for these simple exposure conditions are also lowest for this scenario. These “simple exposure” ages are  $\sim 34\text{--}120 \text{ ka}$  for Duoptečohkka and  $\sim 82\text{--}250 \text{ ka}$  for Tarfalatjårro for the range of erosion rates up to where the ages become asymptotic (Table 2; Fig. 7).

When intermittent surface burial by glacial ice is introduced, maximum erosion rates decrease to  $\sim 17.5 \text{ mm ka}^{-1}$  and  $\sim 7.1 \text{ mm ka}^{-1}$  for Duoptečohkka and Tarfalatjårro, respectively (“burial, 0 isostasy” lines in Fig. 7). Total surface histories also increase for a given erosion rate up to the erosion rate where the ages become asymptotic. These ages vary from 110 to  $\sim 280 \text{ ka}$  and 166 to  $\sim 370 \text{ ka}$  for Duoptečohkka and Tarfalatjårro, respectively.

Increasing by 10% the duration of each period of surface burial by glacial ice has negligible impact on maximum erosion rates for either summit (“10% more burial, isostasy” in Fig. 7). However, long burial periods are reached on Duoptečohkka at lower surface erosion rates than otherwise occurs, resulting in longer total surface histories at these erosion rates. For example, at an erosion rate of  $8 \text{ mm ka}^{-1}$ , the total surface history of Duoptečohkka increases from 123 ka to 199 ka. A similar effect is induced by increasing the duration of snow cover from seven to ten months a year and the depth of snow from 30 cm to 50 cm (“burial, isostasy, more snow” lines in Fig. 7). In addition, increasing the duration and depth of snow cover decreases maximum erosion rates. These values are now  $\sim 15.7 \text{ mm ka}^{-1}$  for Duoptečohkka and  $\sim 6.3 \text{ mm ka}^{-1}$  for Tarfalatjårro.

In summary, the summits of both Duoptečohkka and Tarfalatjårro appear to have been repeatedly inundated by glacial ice over the past 1.07 Ma. The durations of burial and depths of glacial isostatic depression have had notable impacts on total surface

history lengths for each summit. It remains likely, however, that the residence times of regolith mantles on both summits are confined to the late Quaternary. Modelled maximum erosion rates are  $\sim 16.2 \text{ mm ka}^{-1}$  and  $\sim 6.7 \text{ mm ka}^{-1}$  for Duoptečohkka and Tarfalatjårro, respectively.

## 5 Discussion

Minimal chemical weathering of blockfields in the northern Swedish mountains is indicated by the following fine-matrix characteristics: clay-silt ratios  $< 0.5$  in all samples ( $n = 16$ ), the presence of mixed primary and secondary minerals in clay-sized regolith ( $n = 16$ ), and a scarcity of chemically-etched grains in bulk fine matrix (Table 1; Figs. 2–5). In addition, soil horizons and saprolite are absent from all blockfield sections (Table A.1). These findings support those from Goodfellow et al. (2009) and their model of blockfield formation, primarily through physical weathering processes. Conversely, the data does not support blockfield initiation through intense chemical weathering under a warm Neogene climate.

Chemical weathering intensity, although low all-over, varies predictably along hillslope transects. Convex summit areas are the least chemically weathered, as indicated by the absence of well-crystallized secondary minerals (Table 1). This is possibly because these areas are drier (Table A.1) or because fine matrix may not be resident on summits long enough, before being transported downslope, for secondary minerals to become well-crystallized. Vermiculization and gibbsite crystallization in concave locations, such as at the Alddasčorru slope base and the Tarfalatjårro saddle, exhibit the highest chemical weathering intensity. This may be attributable to longer residence times within the blockfields of fine matrix that has been transported downslope, wetter conditions, and/or changes in bedrock mineralogy (Table A.1). The relative paucity of summit fine matrix (Table A.1), which also displays lowest chemical weathering (Table 1; Fig. 4), might therefore indicate recent erosion through, for example, surface creep and subsurface water flow. Altitudinal differences along the transects are gener-

### Arctic-alpine blockfields in northern Sweden

B. W. Goodfellow et al.

Title Page

Abstract

Introduction

Conclusions

References

Tables

Figures

◀

▶

◀

▶

Back

Close

Full Screen / Esc

Printer-friendly Version

Interactive Discussion



ally too small for weathering variations to be clearly related to temperature changes, particularly along the 73 m Tarfalatjårro transect (Fig. 1). However, a slightly milder temperature regime and an extensive grass cover may enhance chemical weathering of the colluvium-till mixture at the base of the Duoštečohkka transect (270 m below the summit), which contains vermiculized minerals and gibbsite (Table 1).

The presence of gibbsite does not indicate a Neogene deep weathering origin of blockfields. Gibbsite is present in up to 10 blockfield samples taken from slopes and saddles and in two of the three mixed till-colluvium samples (Table 1). It is, however, absent from all five summit samples, one slope sample, and the three till samples (Table 1). This distribution of gibbsite indicates that its crystallization is a slow process that extends beyond the Holocene to earlier ice-free periods. However, the presence of gibbsite remains consistent with a blockfield origin under climatic conditions that are seasonally periglacial. Its formation under these conditions can be explained by relatively high local leaching intensities when liquid water is present along spatially heterogeneous flow paths in blockfield regoliths (Meunier et al., 2007; Goodfellow, 2012). A general absence of macrovegetation on high latitude alpine blockfields maintains a slightly acidic pH in regolith pore waters that is also favourable to gibbsite crystallization (Reynolds, 1971; May et al., 1979). Gibbsite can therefore likely form in blockfields within a Quaternary timeframe.

Present surface erosion rates on the Duoštečohkka and Tarfalatjårro summits are low. These values are  $16.2 \text{ mm ka}^{-1}$  (with a range of  $15.7\text{--}18.2 \text{ mm ka}^{-1}$  for the modelled scenarios) and  $6.7 \text{ mm ka}^{-1}$  (with a range of  $6.3\text{--}7.3 \text{ mm ka}^{-1}$  for the modelled scenarios) for Duoštečohkka and Tarfalatjårro, respectively (Fig. 7). The higher erosion rate for Duoštečohkka likely reflects enhanced regolith transport across the narrow, steeply-sided, summit ridgeline. This is perhaps indicated by a patchy regolith only a few 10 s of centimetres thick and by older bedrock apparent surface exposure durations from relict non-glacial surfaces on a nearby part of Alddasčorru (1380 m a.s.l.) and on Olmáčohkka (1355 m a.s.l.) of  $42.1 \pm 2.5$  and  $58.2 \pm 3.5 \text{ ka}$  (analytical errors only), respectively (Fig. 1; Fabel et al., 2002; Stroeven et al., 2006). The lower erosion

**Arctic-alpine  
blockfields in  
northern Sweden**

B. W. Goodfellow et al.

Title Page

Abstract

Introduction

Conclusions

References

Tables

Figures

◀

▶

◀

▶

Back

Close

Full Screen / Esc

Printer-friendly Version

Interactive Discussion



## Arctic-alpine blockfields in northern Sweden

B. W. Goodfellow et al.

Title Page

Abstract

Introduction

Conclusions

References

Tables

Figures

◀

▶

◀

▶

Back

Close

Full Screen / Esc

Printer-friendly Version

Interactive Discussion



rate for the broad, low gradient summit of Tarfalatjårro is likely towards the minimum limit for blockfield-mantled surfaces in this landscape, and is based on an apparent exposure duration which is similar to one derived from bedrock on nearby Dárfalcohkka (1790 m.a.s.l.) of  $72.6 \pm 4.4$  ka (analytical error only; Fig. 1; Stroeven et al., 2006). Blockfields therefore appear to represent end-stage landforms (Boelhouwers, 2004) that effectively armour low-gradient surfaces, making them resistant to erosion and limiting further modification of surface morphology and regolith composition and thickness.

While average erosion rates of blockfield-mantled summits are low, they are of sufficient magnitude to remove shallow (1–2 m thick) regolith profiles within a late Quaternary timeframe, even accounting for periods of surface protection during burial by cold-based glacial ice (Figs. 6 and 7). In addition, erosion rates may have been much higher when Neogene weathering mantles, likely displaying a higher degree of chemical weathering, lost their vegetative cover and were subjected to periglaciation during the onset of cold Quaternary climatic conditions and before the formation of blockfields. There is evidence of extensive removal of Neogene regolith during the early Quaternary in the Canadian Arctic (Refsnider and Miller, 2013) and similar processes may have occurred in northern Scandinavia during this period. In combination, erosion rate estimates through measurements of  $^{10}\text{Be}$  inventories in surface regolith and the absence of chemical weathering evidence for remnant Neogene regoliths indicate that the blockfield mantles have a Quaternary origin.

Low erosion rates and regolith residence times extending over multiple glacial-interglacial cycles indicate that low gradient, blockfield-mantled surfaces provide reasonable markers by which to estimate Quaternary glacial erosion volumes in adjacent glacial landscapes. They also provide evidence against the operation of a glacial “buzz-saw” on blockfield-mantled surfaces in high latitude mountains (Nielsen et al., 2009; Steer et al., 2012), which are generally perceived as non-glacial. This is because it appears highly unlikely that autochthonous blockfields would re-form following regolith removal, glacial plucking, and bedrock polishing by glacial erosion. These processes act to reduce water retention against rock surfaces and infiltration of water into rock

(André, 2002; Ericson, 2004; Hall and Phillips, 2006), which are essential for weathering and block production through chemical processes and frost action (Whalley et al., 2004; Dixon and Thorn, 2005; Goodfellow et al., 2009). Low erosion rates and long regolith residence times also discount the operation of a “periglacial buzz-saw” on low-gradient blockfield-mantled surfaces.

These inferences are, however, tempered by outstanding questions of how thick Neogene regoliths were, their composition, and how they have seemingly been comprehensively removed from all landscape elements in the Scandinavian Mountains, including those presently perceived as non-glacial. Detailed examination of the composition of sedimentary units on the Norwegian continental shelf, such as the NAUST and Molo Formations (e.g. Eidvin et al., 2007), offer some promise in resolving these questions. Our inferences are also tempered by likely spatial variations in erosion rates. Erosion of slopes dominated by solifluction and other mass movements is likely to occur at higher rates than diffusion-dominated low-gradient summits. It therefore remains possible that Quaternary periglacial processes have modified non-glacial surface remnants, now mantled by blockfields, to a greater extent than can be easily recognized (Anderson, 2002; Goodfellow, 2007; Berthling and Etzelmüller, 2011).

## 6 Conclusions

Blockfields on three mountains in northern Sweden were examined and none of them appear to be remnants of thick, intensely weathered Neogene weathering profiles, which has been the prevailing opinion. Minor chemical weathering is indicated in each of the three examined blockfields, with predictable differences according to slope position. Average erosion rates of  $\sim 16.2 \text{ mm ka}^{-1}$  and  $\sim 6.7 \text{ mm ka}^{-1}$  are calculated for two blockfield-mantled summits, from concentrations of in situ-produced cosmogenic  $^{10}\text{Be}$  in surface quartz clasts that were inferred not to have been vertically mixed through the regolith. Although low, these erosion rates are of sufficiently high magnitude to remove present blockfield mantles, which appear to be commonly  $< \sim 2 \text{ m}$  thick, within a late-

### Arctic-alpine blockfields in northern Sweden

B. W. Goodfellow et al.

Title Page

Abstract

Introduction

Conclusions

References

Tables

Figures

◀

▶

◀

▶

Back

Close

Full Screen / Esc

Printer-friendly Version

Interactive Discussion



Quaternary timeframe. This finding remains valid even when accounting for temporal variations in  $^{10}\text{Be}$  production rates attributable to glacial isostasy and burial of ground surfaces by snow and cold-based glacial ice. Blockfield mantles appear to be replenished by regolith formation through, primarily physical, weathering processes that have operated during the Quaternary.

Low gradient, blockfield-mantled surfaces provide reasonable markers by which to estimate Quaternary glacial erosion volumes in adjacent glacial landscapes. This is because blockfield erosion rates are sufficiently low for regolith residence times to extend over multiple glacial-interglacial cycles. The persistence of autochthonous blockfields also discounts recent glacial erosion of surfaces mantled by these regoliths. Coupled with a predicted resistance to the re-establishment of autochthonous blockfields on glacially-eroded surfaces, it seems unlikely that a “glacial buzz-saw” has operated on autochthonous blockfield-mantled surfaces in mountain landscapes. However, the apparent absence of any remnants of Neogene regoliths from these surfaces, which contrasts with low blockfield erosion rates, indicates that more efficient periglacial erosion may have occurred during the onset of cold conditions at the Plio–Pleistocene transition, before the formation of blockfields. The quantity and timing of erosion during this period may be resolvable from detailed examination of offshore sediment sequences.

**Supplementary material related to this article is available online at <http://www.earth-surf-dynam-discuss.net/2/47/2014/esurfd-2-47-2014-supplement.pdf>.**

*Acknowledgements.* We thank Ulf Jonsell, Ben Kirk, Damian Waldron, Mark Wareing, and staff at the Tarfala Research Station and Abisko Scientific Research Station for field support, Ann E. Karlsen and Wiesława Koziel (Geological Survey of Norway, Trondheim) for completing the grain size and XRD analyses, Bjørn Willemoes-Wissing (Geological Survey of Norway, Trondheim) for assisting with SEM, Maria Miguens-Rodriguez (SUERC, East Kilbride) for guiding Goodfellow through sample preparation for AMS, and Stewart Freeman for running AMS on sample “Duo 1”. John Gosse, three anonymous journal reviewers and an associate editor are thanked for helpful comments on an earlier version of this manuscript. The Swedish Society for Anthropology and Geography Andréefonden, Axel Lagrelius’ Fond, Hans and Lillemor

**Arctic-alpine  
blockfields in  
northern Sweden**

B. W. Goodfellow et al.

Title Page

Abstract

Introduction

Conclusions

References

Tables

Figures



Back

Close

Full Screen / Esc

Printer-friendly Version

Interactive Discussion



Ahlmanns Fond, C.F. Liljevalchs Fond, Carl Mannerfelts Fond, and Lars Hiertas minne provided funding to Goodfellow, and Swedish Research Council grants 621-2001-2331 and 621-2005-4972, and a PRIME Lab SEED grant provided funding to Stroeven.

## References

- 5 Anderson, R. S.: Near-surface thermal profiles in alpine bedrock: implications for the frost-weathering of rock, *Arctic Alpine Res.*, 30, 362–372, 1998.
- Anderson, R. S.: Modeling the tor-dotted crests, bedrock edges, and parabolic profiles of high alpine surfaces of the Wind River Range, Wyoming, *Geomorphology*, 46, 35–58, 2002.
- André, M. F.: Rates of postglacial rock weathering on glacially scoured outcrops (Abisko-  
10 Riksgränsen area, 68° N), *Geogr. Ann. A*, 84, 139–150, 2002.
- André, M. F.: Do periglacial landscapes evolve under periglacial conditions?, *Geomorphology*, 52, 149–1164, 2003.
- André, M. F., Hall, K., Bertran, P., and Arocena, J.: Stone runs in the Falkland Islands: periglacial or tropical?, *Geomorphology*, 95, 524–543, 2008.
- 15 Balco, G., Stone, J. O., Lifton, N. A., and Dunai, T. J.: A complete and easily accessible means of calculating surface exposure ages or erosion rates from <sup>10</sup>Be and <sup>26</sup>Al measurements, *Quat. Geochronol.*, 3, 174–195, 2008.
- Ballantyne, C. K.: Age and significance of mountain-top detritus, *Permafrost Periglac.*, 9, 327–345, 1998.
- 20 Ballantyne, C. K.: A general model of autochthonous blockfield evolution, *Permafrost Periglac.*, 21, 289–300, 2010.
- Ballantyne, C. K., McCarroll, D., Nesje, A., Dahl, S. O., and Stone, J. O.: The last ice sheet in north-west Scotland: reconstruction and implications, *Quaternary Sci. Rev.*, 17, 1149–1184, 1998.
- 25 Berthling, I. and Etzelmüller, B.: The concept of cryo-conditioning in landscape evolution, *Quaternary Res.*, 75, 378–384, 2011.
- Bierman, P. R., Marsella, K. A., Patterson, C., Davis, P. T., and Caffee, M.: Mid-Pleistocene cosmogenic minimum-age limits for pre-Wisconsinan glacial surfaces in southwestern Minnesota and southern Baffin Island: a multiple nuclide approach, *Geomorphology*, 27, 25–39,  
30 1999.

## Arctic-alpine blockfields in northern Sweden

B. W. Goodfellow et al.

Title Page

Abstract

Introduction

Conclusions

References

Tables

Figures



Back

Close

Full Screen / Esc

Printer-friendly Version

Interactive Discussion



## Arctic-alpine blockfields in northern Sweden

B. W. Goodfellow et al.

Title Page

Abstract

Introduction

Conclusions

References

Tables

Figures

◀

▶

◀

▶

Back

Close

Full Screen / Esc

Printer-friendly Version

Interactive Discussion



- Bintanja, R., van de Wal, R. S. W., and Oerlemans, J.: Global ice volume variations through the last glacial cycle simulated by a 3-D ice-dynamical model, *Quatern. Int.*, 95–96, 11–23, 2002.
- Bintanja, R., van de Wal, R. S. W., and Oerlemans, J.: Modelled atmospheric temperatures and global sea levels over the past million years, *Nature*, 437, 125–128, 2005.
- Boelhouwers, J., Holness, S. Meiklejohn, I., and Sumner, P.: Observations on a blockstream in the vicinity of Sani Pass, Lesotho Highlands, southern Africa, *Permafrost Periglac.*, 13, 251–257, 2002.
- Boelhouwers, J. C.: New perspectives on autochthonous blockfield development, *Polar Geogr.*, 28, 133–146, 2004.
- Brindley, G. W. and Brown, G.: *Crystal Structures of Clay Minerals and their X-ray Identification*, Mineralogical Society, London, 495 pp., 1980.
- Briner, J. P., Miller, G. H., Davis, P. T., Bierman, P. R., and Caffee, M.: Last Glacial Maximum ice sheet dynamics in Arctic Canada inferred from young erratics perched on ancient tors, *Quaternary Sci. Rev.*, 22, 437–444, 2003.
- Caine, N.: *The Blockfields of Northeastern Tasmania*, Publication G/6, Department of Geography, Research School of Pacific Studies, The Australian National University, Canberra, 127 pp., 1968.
- Charbit, S., Ritz, C., Philippon, G., Peyaud, V., and Kageyama, M.: Numerical reconstructions of the Northern Hemisphere ice sheets through the last glacial-interglacial cycle, *Clim. Past*, 3, 15–37, doi:10.5194/cp-3-15-2007, 2007.
- Child, D., Elliott, G., Mifsud, C., Smith, A. M., and Fink, D.: Sample processing for earth science studies at ANTARES, *Nucl. Instrum. Meth. B*, 172, 856–860, 2000.
- Clapperton, C. M.: Further observations on the stone runs of the Falkland Islands, *Biuletyn Peryglacjalny*, 24, 211–217, 1975.
- Cockburn, H. A. P. and Summerfield, M. A.: Geomorphological applications of cosmogenic isotope analysis, *Prog. Phys. Geog.*, 28, 1–42, 2004.
- Dahl, R.: Block fields, weathering pits and tor-like forms in the Narvik mountains, Nordland, Norway, *Geogr. Ann. A*, 48, 55–85, 1966.
- Dixon, J. C. and Thorn, C. E.: Chemical weathering and landscape development in mid-latitude alpine environments, *Geomorphology*, 67, 127–145, 2005.
- Dredge, L.: Breakup of limestone bedrock by frost shattering and chemical weathering, Eastern Canadian Arctic, *Arctic Alpine Res.*, 24, 314–323, 1992.

## Arctic-alpine blockfields in northern Sweden

B. W. Goodfellow et al.

Title Page

Abstract

Introduction

Conclusions

References

Tables

Figures

◀

▶

◀

▶

Back

Close

Full Screen / Esc

Printer-friendly Version

Interactive Discussion



- Dredge, L. A.: Age and origin of upland block fields on Melville Peninsula, eastern Canadian Arctic, *Geogr. Ann. A*, 82, 443–454, 2000.
- Eidvin, T., Bugge, T., and Smelror, M.: The Molo Formation, deposited by coastal progradation on the inner Mid-Norwegian continental shelf, coeval with the Kai Formation to the west and the Utsira Formation in the North Sea, *Norw. J. Geol.*, 87, 75–142, 2007.
- Ericson, K.: Geomorphological surfaces of different age and origin in granite landscapes: an evaluation of the Schmidt hammer test, *Earth Surf. Proc. Land.*, 29, 495–509, 2004.
- Eriksson, B.: Data rörande Sveriges temperaturklimat (Data concerning the air temperature of Sweden), SMHI Reports, Meteorology and Climatology, RMK 39, 1982.
- Fabel, D., Stroeven, A. P., Harbor, J., Kleman, J., Elmore, D., and Fink, D.: Landscape preservation under Fennoscandian ice sheets determined from in situ produced  $^{10}\text{Be}$  and  $^{26}\text{Al}$ , *Earth Planet. Sc. Lett.*, 201, 397–406, 2002.
- Fjeldskaar, W., Lindholm, C., Dehls, J. F., and Fjeldskaar, I.: Postglacial uplift, neotectonics and seismicity in Fennoscandia, *Quaternary Sci. Rev.*, 19, 1413–1422, 2000.
- Fjellanger, J., Sørbel, L., Linge, H., Brook, E. J., Raisbeck, G. M., and Yiou, F.: Glacial survival of blockfields on the Varanger Peninsula, northern Norway, *Geomorphology*, 82, 255–272, 2006.
- Fredén, C. (Ed): National Atlas of Sweden: Land and Soils, Sveriges Nationalatlas, Vällingby, 208 pp., 2002.
- Glasser, N. and Hall, A.: Calculating Quaternary glacial erosion rates in northeast Scotland, *Geomorphology*, 20, 29–48, 1997.
- Goldstein, J., Newbury, D. E., Joy, D. C., Lyman, C. E., Echlin, P., Lifshin, E., Sawyer, L. C., and Michael, J. R.: Scanning Electron Microscopy and X-ray Microanalysis, 3rd edn., Kluwer Academic/Plenum Publishers, New York, 689 pp., 2003.
- Goodfellow, B. W.: Relict non-glacial surfaces in formerly glaciated landscapes, *Earth-Sci. Rev.*, 80, 47–73, 2007.
- Goodfellow, B. W.: A granulometry and secondary mineral fingerprint of chemical weathering in periglacial landscapes and its application to blockfield origins, *Quaternary Sci. Rev.*, 57, 121–135, 2012.
- Goodfellow, B. W., Stroeven, A. P., Hättestrand, C., Kleman, J., and Jansson, K. N.: Deciphering a non-glacial/glacial landscape mosaic in the northern Swedish mountains, *Geomorphology*, 93, 213–232, 2008.

## Arctic-alpine blockfields in northern Sweden

B. W. Goodfellow et al.

Title Page

Abstract

Introduction

Conclusions

References

Tables

Figures

◀

▶

◀

▶

Back

Close

Full Screen / Esc

Printer-friendly Version

Interactive Discussion



- Goodfellow, B. W., Fredin, O., Derron, M.-H., and Stroeven, A. P.: Weathering processes and Quaternary origin of an alpine blockfield in Arctic Sweden, *Boreas*, 38, 379–398, 2009.
- Granger, D. E., Riebe, C. S., Kirchner, J. W., and Finkel, R. C.: Modulation of erosion on steep granitic slopes by boulder armoring, as revealed by cosmogenic  $^{26}\text{Al}$  and  $^{10}\text{Be}$ , *Earth Planet. Sc. Lett.*, 186, 269–281, 2001.
- Grudd, H. and Schneider, T.: Air temperature at Tarfala Research Station 1946–1995, *Geogr. Ann. A*, 78A, 115–119, 1996.
- Hall, A. M. and Phillips, W. M.: Weathering pits as indicators of the relative age of granite surfaces in the Cairngorm Mountains, Scotland, *Geogr. Ann. A*, 88, 135–150, 2006.
- Hättestrand, C. and Stroeven, A. P.: A relict landscape in the centre of Fennoscandian glaciation; geomorphological evidence of minimal Quaternary glacial erosion, *Geomorphology*, 44, 127–143, 2002.
- Isaksen, K., Holmlund, P., Sollid, J. L., and Harris, C.: Three deep alpine-permafrost boreholes in Svalbard and Scandinavia, *Permafrost Periglac.*, 12, 13–25, 2001.
- Isaksen, K., Sollid, J. L., Holmlund, P., and Harris, C.: Recent warming of mountain permafrost in Svalbard and Scandinavia, *J. Geophys. Res.*, 112, F02S04, doi:10.1029/2006JF000522, 2007.
- Ives, J. D.: Block fields, associated weathering forms on mountain tops and the Nunatak hypothesis, *Geogr. Ann. A*, 4, 220–223, 1966.
- Ives, J. D.: Biological refugia and the nunatak hypothesis, in: *Arctic and Alpine Environments*, edited by: Ives, J. D. and Barry, R. G., Methuen, London, 605–636, 1974.
- Jansson, K. N., Stroeven, A. P., Alm, G., Dahlgren, K. I. T., Glasser, N. F., and Goodfellow, B. W.: Using a GIS filtering approach to replicate patterns of glacial erosion, *Earth Surf. Proc. Land.*, 36, 408–418, 2011.
- Kauffman, G., Wu, P., and Li, G.: Glacial isostatic adjustment in Fennoscandia for a laterally heterogeneous earth, *Geophys. J. Int.*, 143, 262–273, 2000.
- Kleman, J. and Stroeven, A. P.: Preglacial surface remnants and Quaternary glacial regimes in northwestern Sweden, *Geomorphology*, 19, 35–54, 1997.
- Kleman, J., Stroeven, A. P., and Lundqvist, J.: Patterns of Quaternary ice sheet erosion and deposition in Fennoscandia and a theoretical framework for explanation, *Geomorphology*, 97, 73–90, 2008.
- Kohl, C. P. and Nishiizumi, K.: Chemical isolation of quartz for measurement of in situ-produced cosmogenic nuclides, *Geochim. Cosmochim. Ac.*, 56, 3586–3587, 1992.

## Arctic-alpine blockfields in northern Sweden

B. W. Goodfellow et al.

Title Page

Abstract

Introduction

Conclusions

References

Tables

Figures

◀

▶

◀

▶

Back

Close

Full Screen / Esc

Printer-friendly Version

Interactive Discussion



- Lal, D.: Cosmic ray labeling of erosion surfaces: in situ nuclide production rates and erosion models, *Earth Planet. Sc. Lett.*, 104, 424–439, 1991.
- Lambeck, K., Purcell, A., Funder, S., Kjør, K. H., Larsen, E., and Möller, P.: Constraints on the Late Saalian to early Middle Weichselian ice sheet of Eurasia from field data and rebound modeling, *Boreas*, 35, 539–575, 2006.
- Le Meur, E. and Huybrechts, P.: A comparison of different ways of dealing with isostasy: examples from modelling the Antarctic ice sheet during the last glacial cycle, *Ann. Glaciol.*, 23, 309–317, 1996.
- Li, Y., Fabel, D., Stroeven, A. P., and Harbor, J.: Unraveling complex exposure-burial histories of bedrock surfaces under ice sheets by integrating cosmogenic nuclide concentrations with climate proxy records, *Geomorphology*, 99, 139–149, 2008.
- Lisiecki, L. E. and Raymo, M. E.: A Pliocene-Pleistocene stack of 57 globally distributed benthic  $\delta^{18}\text{O}$  records, *Paleoceanography*, 20, PA1003, doi:10.1029/2004PA001071, 2005.
- Marquette, G. C., Gray, J. T., Gosse, J. C., Courchesne, F., Stockli, L., MacPherson, G., and Finkel, R.: Felsenmeer persistence under non-erosive ice in the Torngat and Kaumajet mountains, Quebec and Labrador, as determined by soil weathering and cosmogenic nuclide exposure dating, *Can. J. Earth Sci.*, 41, 19–38, 2004.
- May, H. M., Helmke, P. A., and Jackson, M. L.: Gibbsite solubility and thermodynamic properties of hydroxy-aluminum ions in aqueous solution at 25 °C, *Geochim. Cosmochim. Ac.*, 43, 861–868, 1979.
- Meunier, A., Sardini, P., Robinet, J. C., and Pret', D.: The petrography of weathering processes: facts and outlooks, *Clay Miner.*, 42, 415–435, 2007.
- Migoñ, P.: *Granite Landscapes of the World*, Oxford University Press, Oxford, UK, 2006.
- Milne, G. A., Mitrovica, J. X., Scherneck, H.-G., Davis, J. L., Johansson, J. M., Koivula, H., and Vermeer, M.: Continuous GPS measurements of postglacial adjustment in Fennoscandia: 2. Modelling results, *J. Geophys. Res.*, 109, 1–18, 2004.
- Moore, D. M. and Reynolds, R. C.: *X-ray Diffraction and the Identification and Analysis of Clay Minerals*, 2nd edn., University Press, Oxford, 378 pp., 1997.
- Nesje, A. and Whillans, I. M.: Erosion of Sognefjord, Norway, *Geomorphology*, 9, 33–45, 1994.
- Nesje, A., Dahl, S. O., Anda, E., and Rye, N.: Block fields in southern Norway: significance for the Late Weichselian ice sheet, *Norsk Geolog. Tidsskr.*, 68, 149–169, 1988.
- Nielsen, S. B., Gallagher, K., Leighton, C., Balling, N., Svenningsen, L., Jacobsen, B. H., Thomsen, E., Nielsen, O. B., Heilmann-Clausen, C., Egholm, D. L., Summerfield, M. A.,

## Arctic-alpine blockfields in northern Sweden

B. W. Goodfellow et al.

Title Page

Abstract

Introduction

Conclusions

References

Tables

Figures

◀

▶

◀

▶

Back

Close

Full Screen / Esc

Printer-friendly Version

Interactive Discussion



- Clausen, O. R., Piotrowski, J. A., Thorsen, M. R., Huuse, M., Abrahamsen, N., King, C., and Lykke-Andersen, H.: The evolution of western Scandinavian topography: a review of Neogene uplift versus the ICE (isostasy-climate-erosion) hypothesis, *J. Geodyn.*, 47, 72–95, 2009.
- 5 Nishiizumi, K.: Preparation of  $^{26}\text{Al}$  AMS standards, *Nucl. Instrum. Meth. B*, 223–224, 388–392, 2004.
- Nishiizumi, K., Imamura, M., Caffee, M. W., Southern, J. R., Finkel, R. C., and McAninch, J.: Absolute calibration of  $^{10}\text{Be}$  AMS standards, *Nucl. Instrum. Meth. B*, 258, 403–413, 2007.
- Paasche, Ø., Strømsøe, J. R., Dahl, S. O., and Linge, H.: Weathering characteristics of arctic islands in northern Norway, *Geomorphology*, 82, 430–452, 2006.
- 10 Peltier, W. R.: Ice age paleotopography, *Science*, 265, 195–201, 1994.
- Peltier, W. R.: Global glacial isostasy and the surface of the ice-age Earth: the ICE-5G (VM2) Model and GRACE, *Annu. Rev. Earth Pl. Sc.*, 32, 111–149, 2004.
- Phillips, W. M., Hall, A. M., Mottram, R., Fifield, L. K., and Sugden, D.: Cosmogenic  $^{10}\text{Be}$  and  $^{26}\text{Al}$  exposure ages of tors and erratics, Cairngorm Mountains, Scotland: Timescales for the development of a classic landscape of selective linear glacial erosion, *Geomorphology*, 73, 224–245, 2006.
- 15 Potter, N. and Moss, J. H.: Origin of the Blue Rocks block field and adjacent deposits, Berks County, Pennsylvania, *Geol. Soc. Am. Bull.*, 79, 255–262, 1968.
- Rea, B. R.: Blockfields (Felsenmeer), in: *The Encyclopedia of Quaternary Science*, vol. 3, edited by: Elias, S. A., Elsevier, Amsterdam, 523–534, 2013.
- 20 Rea, B. R., Whalley, B., Rainey, M. M., and Gordon, J. E.: Blockfields, old or new? Evidence and implications from some plateaus in northern Norway, *Geomorphology*, 15, 109–121, 1996.
- Refsnider, K. A. and Miller, G. H.: Ice-sheet erosion and the stripping of Tertiary regolith from Baffin Island, eastern Canadian Arctic, *Quaternary Sci. Rev.*, 67, 176–189, 2013.
- 25 Reynolds, R. C.: Clay mineral formation in an alpine environment, *Clay. Clay Miner.*, 19, 361–374, 1971.
- Small, E. E., Anderson, R. S. Repka, J. L. and Finkel, R.: Erosion rates of alpine bedrock summit surfaces deduced from in situ  $^{10}\text{Be}$  and  $^{26}\text{Al}$ , *Earth Planet. Sc. Lett.*, 150, 413–425, 1997.
- 30 Small, E. E., Anderson, R. S., and Hancock, G. S.: Estimates of the rate of regolith production using  $^{10}\text{Be}$  and  $^{26}\text{Al}$  from an alpine hillslope, *Geomorphology*, 27, 131–150, 1999.

## Arctic-alpine blockfields in northern Sweden

B. W. Goodfellow et al.

Title Page

Abstract

Introduction

Conclusions

References

Tables

Figures

◀

▶

◀

▶

Back

Close

Full Screen / Esc

Printer-friendly Version

Interactive Discussion



- Staiger, J. K. W., Gosse, J. C., Johnson, J. V., Fastook, J., Gray, J. T., Stockli, D. F., Stockli, L., and Finkel, R.: Quaternary relief generation by polythermal glacier ice, *Earth Surf. Proc. Land.*, 30, 1145–1159, 2005.
- Steer, P., Huismans, R. S., Valla, P. G., Gac, S., and Herman, F.: Bimodal Plio–Quaternary glacial erosion of fjords and low-relief surfaces in Scandinavia, *Nat. Geosci.*, 5, 635–639, 2012.
- Steffen, H. and Kauffman, G.: Glacial isostatic adjustment of Scandinavia and northwestern Europe and the radial viscosity structure of the Earth’s mantle, *Geophys. J. Int.*, 163, 801–812, 2005.
- Steffen, H., Kauffman, G., and Wu, P.: Three-dimensional finite-element modeling of the glacial isostatic adjustment in Fennoscandia, *Earth Planet. Sc. Lett.*, 250, 358–375, 2006.
- Stone, J. O.: Air pressure and cosmogenic isotope production, *J. Geophys. Res.*, 105, 23753–23759, 2000.
- Stroeven, A. P., Fabel, D., Hattestrand, C., and Harbor, J.: A relict landscape in the centre of Fennoscandian glaciation; cosmogenic radionuclide evidence of tors preserved through multiple glacial cycles, *Geomorphology*, 44, 145–154, 2002.
- Stroeven, A. P., Harbor, J., Fabel, D., Kleman, J., Hättestrand, C. Elmore, D., Fink, D., and Fredin, O.: Slow, patchy landscape evolution in northern Sweden despite repeated ice-sheet glaciation, *Geological Society of America Special Paper*, 398, 387–396, 2006.
- Strømsøe, J. R. and Paasche, Ø: Weathering patterns in high-latitude regolith, *J. Geophys. Res.*, 116, F03021, doi:10.1029/2010JF001954, 2011.
- Sugden, D. E.: The selectivity of glacial erosion in the Cairngorm Mountains, Scotland, *T. I. Brit. Geogr.*, 45, 79–92, 1968.
- Sugden, D. E.: Landscapes of glacial erosion in Greenland and their relationship to ice, topographic and bedrock conditions, in: *Progress in Geomorphology: Papers in honour of D. L. Linton*, edited by: Brown, E. H. and Waters, R. S., Institute of British Geographers Special Publication, vol. 7, 177–195, 1974.
- Sugden, D. E. and Watts, S. H.: Tors, felsenmeer, and glaciation in northern Cumberland Peninsula, Baffin Island, *Can. J. Earth Sci.*, 14, 2817–2823, 1977.
- Sumner, P. D. and Meiklejohn, K. I.: On the development of autochthonous blockfields in the grey basalts of sub-Antarctic Marion Island, *Polar Geogr.*, 28, 120–132, 2004.
- US Department of Agriculture: Soil Survey Manual, Agricultural Handbook No. 18, Government Printing Office, Washington DC, 532 pp., 1993.

Whalley, W. B., Rea, B. R., and Rainey, M.: Weathering, blockfields, and fracture systems and the implications for long-term landscape formation: some evidence from Lyngen and Øksfordjøkelen areas in north Norway, *Polar Geogr.*, 28, 93–119, 2004.

- 5 White, A. F., Blum, A. E., Schulz, M. S., Vivit, D. V., Stonestrom, D. A., Larsen, M., Murphy, S. F., and Eberl, D.: Chemical weathering in a tropical watershed, Luquillo Mountains, Puerto Rico: I. Long-term versus short-term weathering fluxes, *Geochim. Cosmochim. Ac.*, 62, 209–226, 1998.

# ESURFD

2, 47–93, 2014

## Arctic-alpine blockfields in northern Sweden

B. W. Goodfellow et al.

Title Page

Abstract

Introduction

Conclusions

References

Tables

Figures



Back

Close

Full Screen / Esc

Printer-friendly Version

Interactive Discussion



**Table 1.** Particle size distribution and secondary minerals in fine matrix from Alddasčorru, Duoptečohkka, and Tarfalaťjårro transects, and from Ruohtahakčorru and Nulpotjåkka summit tills.

Transect and pit	Sample <sup>a</sup>	Location <sup>b</sup> (process unit)	Elevation (m.a.s.l.)	Depth (m)	Clay (%)	Silt (%)	Sand (%)	Clay/ Silt	Clay Minerals <sup>c</sup>
Alddasčorru 1	BG-05-11	Summit (1)	1538	Surface	4.9	42.2	52.9	0.12	C, I, A, P, Q
Alddasčorru 1	BG-05-04	Summit (1)	1538	0.16	3.4	29.3	67.3	0.12	C, I, A, P, Q
Alddasčorru 1	BG-05-16	Summit (1)	1538	0.60	2.7	23.6	73.7	0.11	C, I, A, P, Q
Alddasčorru 2	BG-05-26	Slope (1)	1500	0.60	4.5	36.2	59.4	0.12	C, I, A, G?, P, Q
Alddasčorru 5	BG-05-67	Slope base (3)	1260	0.40	5.8	46.5	47.7	0.12	C, V, I, A, G, P, Q
Alddasčorru 6	BG-05-68	Slope base (3)	1260	0.40	4.1	37.0	58.8	0.11	C, V, I, A, G, P, Q
Alddasčorru 7	BG-05-69	Slope base (3)	1260	0.40	3.2	29.2	67.6	0.11	C, V, I, A, G, P, Q
Duoptečohkka 5	BG-05-64	Slope (2)	1200	0.40	4.0	40.6	55.4	0.10	C, V, I, A, P, Q
Duoptečohkka 6	BG-05-65	Slope (2)	1200	0.40	4.1	40.3	55.6	0.10	C, V, I, A, G, P, Q
Duoptečohkka 7	BG-05-66	Slope (2)	1200	0.40	4.4	38.4	57.3	0.11	C, V, I, A, G?, P, Q
Duoptečohkka 8	BG-05-70	Colluvium/till (4)	1060	0.40	1.1	14.1	84.8	0.08	C, V, I, A, P, Q
Duoptečohkka 9	BG-05-71	Colluvium/till (4)	1060	0.40	3.6	34.1	62.3	0.11	C, V, I, A, G, P, Q
Duoptečohkka 10	BG-05-72	Colluvium/till (4)	1060	0.40	1.5	20.8	77.7	0.07	C, V, I, A, G?, P, Q
Tarfalaťjårro 1	BG-04-25	Summit (1)	1626	1.25	1.5	39.5	59.0	0.04	C, I, A, P, Q
Tarfalaťjårro 2	BG-06-22	Summit (1)	1626	Surface	5.6	39.3	55.2	0.14	C, I, A, P, Q
Tarfalaťjårro 3	BG-04-26	Summit/slope (1)	1623	0.80	2.1	45.5	52.4	0.05	C, I, A, P, Q
Tarfalaťjårro 6	BG-05-83	Saddle (1)	1553	0.50	4.7	41.3	54.0	0.11	C, V, I, A, G, P, Q
Tarfalaťjårro 7	BG-05-84	Saddle (1)	1553	0.20	5.3	49.9	44.8	0.11	C, V, I, A, G, P, Q
Tarfalaťjårro 8	BG-05-85	Saddle (1)	1553	0.20	5.4	49.8	44.8	0.11	C, V, I, A, G, P, Q
Tarfalaťjårro 9	BG-06-07	Saddle (1)	1553	0.70	5.4	46.1	48.5	0.12	C, V, I, A, G, P, Q
Ruohtahakčorru	BG-04-22	Summit till	1342	0.50	2.2	52.8	45.0	0.04	C, V, I, A, P, Q
Ruohtahakčorru	BG-04-23	Summit till	1346	0.90	0.7	10.3	89.0	0.07	C, V, I, A, P, Q
Ruohtahakčorru	BG-04-24	Summit till	1343	1.20	2.6	37.7	59.7	0.07	C, V, I, A, P, Q
Nulpotjåkka	BG-04-27	Summit till	1405	0.90	0.7	47.2	52.1	0.01	C, V, I, A, P, Q

<sup>a</sup> BG-06-22 and BG-06-07 are representative of eight samples from Tarfalaťjårro pit 2 and seven samples from Tarfalaťjårro pit 9, respectively (Goodfellow et al., 2009).

<sup>b</sup> Process units are numbered as follows: (1) diffusion-dominated summit, (2) solifluction-dominated slope, (3) solifluction-shallow landsliding-tumbling blocks, (4) concave depositional where regolith comprises colluvium and till. Till is indicated by the presence of clasts of different lithologies and an abundance of fine matrix.

<sup>c</sup> C = chlorite; V = vermiculite; I = illite; A = amphibole; G = gibbsite (? indicates uncertain); P = plagioclase (dominant feldspar); Q = quartz.

## Arctic-alpine blockfields in northern Sweden

B. W. Goodfellow et al.

Title Page

Abstract

Introduction

Conclusions

References

Tables

Figures

◀

▶

◀

▶

Back

Close

Full Screen / Esc

Printer-friendly Version

Interactive Discussion



## Arctic-alpine blockfields in northern Sweden

B. W. Goodfellow et al.

Title Page

Abstract

Introduction

Conclusions

References

Tables

Figures

◀

▶

◀

▶

Back

Close

Full Screen / Esc

Printer-friendly Version

Interactive Discussion



**Table 2.** Cosmogenic nuclide data, apparent exposure ages, and nuclide ratios.

Sample <sup>a</sup>	Location (° N/° E)	Elevation (m a.s.l.)	Thickness <sup>b</sup> (cm)	Shielding Factor	Quartz (g)	Be carrier (mg)	<sup>10</sup> Be/ <sup>9</sup> Be <sup>c</sup> (×10 <sup>-13</sup> )	[ <sup>10</sup> Be] <sup>c, d, e, f</sup> (10 <sup>6</sup> atoms g <sup>-1</sup> )	Al carrier (mg)	<sup>26</sup> Al/ <sup>27</sup> Al <sup>c</sup> (×10 <sup>-13</sup> )	[ <sup>26</sup> Al] <sup>c, f, g, h</sup> (10 <sup>6</sup> atoms g <sup>-1</sup> )
Duo 1	68.42/19.37	1330	3	1.0000	41.8211	0.3094	11.40 ± 0.30	0.51 ± 0.02	0.7222	50.10 ± 1.05	3.52 ± 0.19
Tar 1	67.61/18.52	1626	4	0.9998	54.2814	0.2741	44.70 ± 1.20	1.55 ± 0.05	0.9028	170.00 ± 6.00	9.59 ± 0.59

## Arctic-alpine blockfields in northern Sweden

B. W. Goodfellow et al.

Table 2. Continued.

<sup>10</sup> Be apparent age <sup>c, ij</sup> (ka)		<sup>26</sup> Al apparent age <sup>c, ij</sup> (ka)		<sup>26</sup> Al/ <sup>10</sup> Be <sup>c</sup> ratio	
Age ±1σ (int)	±1σ (ext)	Age ±1σ (int)	±1σ (ext)		
	33.5 ± 1.2	±3.2	32.7 ± 1.8	±3.4	6.57 ± 0.43
	81.8 ± 2.8	±7.8	72.6 ± 4.6	±8.0	5.92 ± 0.41

<sup>a</sup> Duo 1 = surface sample from Duoptečohkka pit 1; Tar 1 = surface sample from Tarfalatjårro pit 1.

<sup>b</sup> A quartzite density of 2.65 g cm<sup>-3</sup> was used for thickness corrections.

<sup>c</sup> Uncertainties are reported at the 1σ confidence level.

<sup>d</sup> Measured <sup>10</sup>Be concentrations were normalized to NIST SRM 4325, with a <sup>10</sup>Be/<sup>9</sup>Be ratio of 2.79 ± 0.03 × 10<sup>-11</sup> and using a <sup>10</sup>Be half-life of 1.36 × 10<sup>6</sup> a (Nishiizumi et al., 2007).

<sup>e</sup> Blank values of 115 436 ± 37 556 <sup>10</sup>Be atoms (<sup>10</sup>Be/<sup>9</sup>Be = 6.6 × 10<sup>-15</sup> ± 1.6 × 10<sup>-15</sup>) and 56 776 ± 39 917

<sup>10</sup>Be atoms (<sup>10</sup>Be/<sup>9</sup>Be = 4.1 × 10<sup>-15</sup> ± 2.0 × 10<sup>-15</sup>) were used to correct for background in Duoptečohkka 1 and Tarfalatjårro 1, respectively.

<sup>f</sup> Propagated uncertainties include error in the blank, carrier mass (1%), and counting statistics.

<sup>g</sup> Measured <sup>26</sup>Al concentrations were normalized to PRIME standard Z92-0222 with a nominal <sup>26</sup>Al/<sup>27</sup>Al ratio of 4.11 × 10<sup>-11</sup> and using an <sup>26</sup>Al half-life of 7.05 × 10<sup>5</sup> a (Nishiizumi, 2004).

<sup>h</sup> Blank values of 337 056 ± 99 378 <sup>26</sup>Al atoms (<sup>26</sup>Al/<sup>27</sup>Al = 11.4 × 10<sup>-15</sup> ± 3.3 × 10<sup>-15</sup>) and

183 701 ± 275 552 <sup>26</sup>Al atoms (<sup>26</sup>Al/<sup>27</sup>Al = 6.0 × 10<sup>-15</sup> ± 9.0 × 10<sup>-15</sup>) were used to correct for background in Duoptečohkka 1 and Tarfalatjårro 1, respectively.

<sup>i</sup> Apparent exposure ages were calculated using the CRONUS-Earth calculator (version 2.2; Balco et al., 2008). Constant (time-invariant) <sup>10</sup>Be and <sup>26</sup>Al spallogenic production rate models (Lal, 1991; Stone, 2000) were used. Muogenic production was also incorporated into the production rate models giving total

<sup>10</sup>Be production rates of 16.138 atoms g<sup>-1</sup> a<sup>-1</sup> for Duoptečohkka 1 and 20.196 atoms g<sup>-1</sup> a<sup>-1</sup> for

Tarfalatjårro 1. Total <sup>26</sup>Al production rates are 109.368 atoms g<sup>-1</sup> a<sup>-1</sup> for Duoptečohkka 1 and

136.788 atoms g<sup>-1</sup> a<sup>-1</sup> for Tarfalatjårro 1.

<sup>j</sup> (int) = internal (analytical) uncertainties; (ext) = propagated external uncertainties (Balco et al., 2008).

Title Page

Abstract

Introduction

Conclusions

References

Tables

Figures

◀

▶

◀

▶

Back

Close

Full Screen / Esc

Printer-friendly Version

Interactive Discussion



## Arctic-alpine blockfields in northern Sweden

B. W. Goodfellow et al.

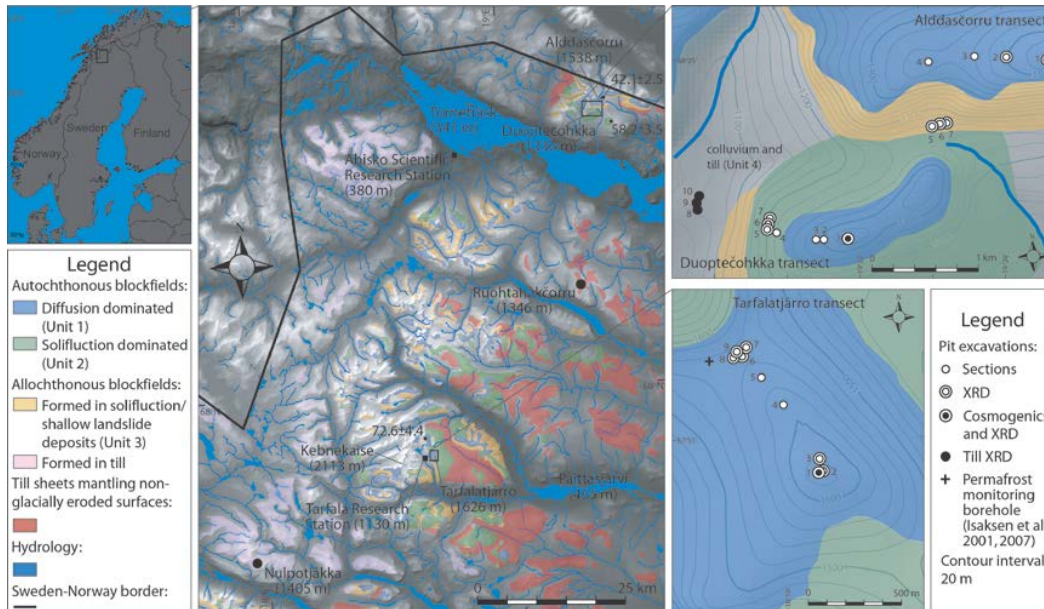
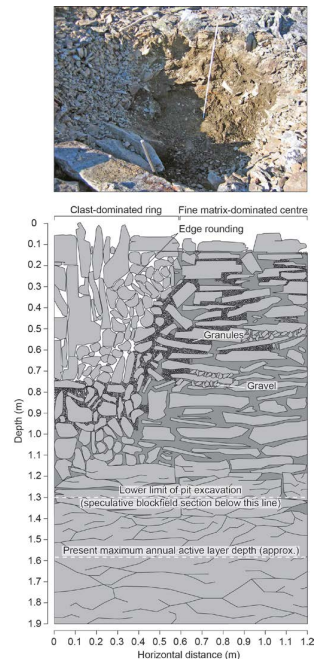


Fig. 1. Caption on next page.



## Arctic-alpine blockfields in northern Sweden

B. W. Goodfellow et al.



**Fig. 2.** Representative vertical sections of autochthonous blockfields. The photograph shows an excavation across a sorted circle developed in the summit blockfield of Tarfalatjärro and the line drawing summarizes the general features of autochthonous blockfields in a vertical section cut across a periglacially sorted circle. The ruler in the photograph is 1 m in length. Angular cobbles and boulders are embedded in fine matrix (clay, silt, sand) in sorted circle centres. Granules and gravel accumulate between clasts distributed vertically through the section that have horizontally-oriented long axes. Conversely the outer ring of the sorted circle is comprised of gravel, cobbles and boulders, while granules accumulate near the base of the section. Clast surfaces are sub-rounded where they are subaerially exposed. The pit bases intersect large slabs and are wet.

Title Page

Abstract

Introduction

Conclusions

References

Tables

Figures

◀

▶

◀

▶

Back

Close

Full Screen / Esc

Printer-friendly Version

Interactive Discussion



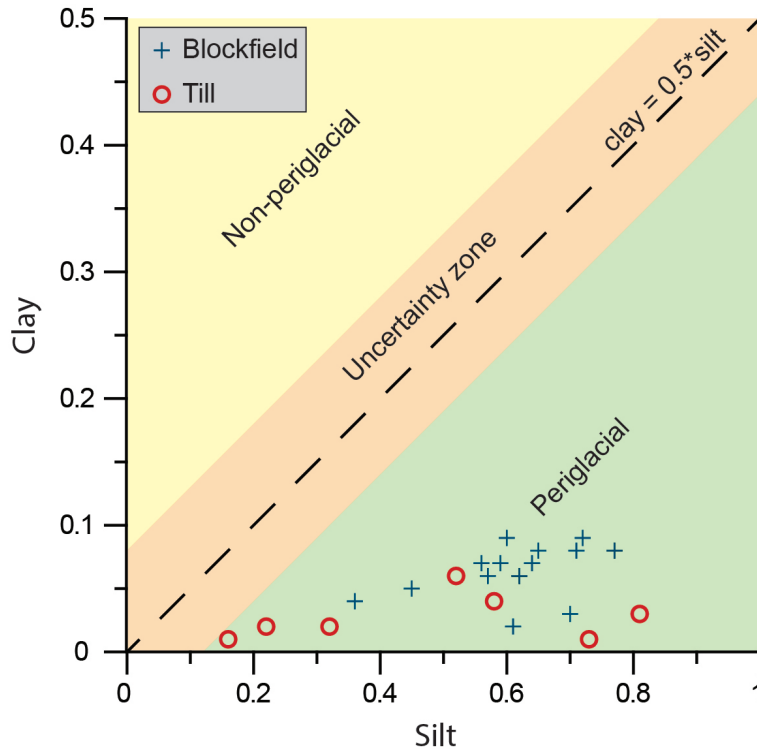


**Fig. 3.** Quantities of clay and silt in fine matrix samples collected from blockfields (blue crosses) and till (red circles). All samples contain clay-silt ratios less than 0.5, which indicates fine matrix production under conditions that have been, at least seasonally, periglacial (Goodfellow, 2012). All data (in percentage) have been divided by 65 to fit on 0–1 scales. Fine matrix samples falling in the uncertainty zone may, or may not, have been exposed to periglacial conditions during their formation (Goodfellow, 2012).

**Arctic-alpine  
blockfields in  
northern Sweden**

B. W. Goodfellow et al.

Title Page

Abstract

Introduction

Conclusions

References

Tables

Figures

◀

▶

◀

▶

Back

Close

Full Screen / Esc

Printer-friendly Version

Interactive Discussion



## Arctic-alpine blockfields in northern Sweden

B. W. Goodfellow et al.

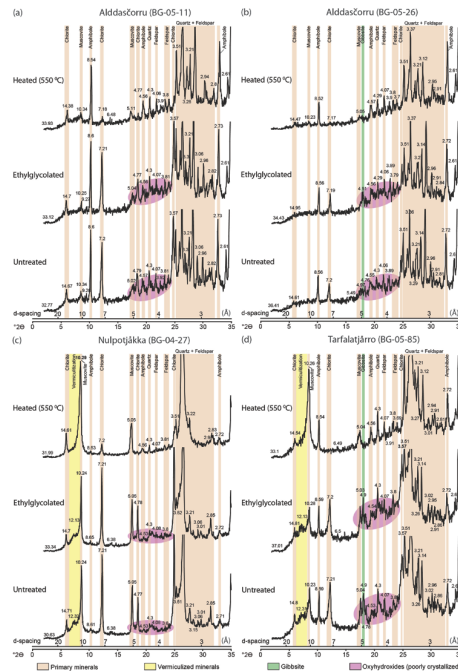


**Fig. 4.** Four representative X-ray diffractograms of the clay-sized fraction ( $< 2 \mu\text{m}$ ) of fine matrix samples from: **(a)** Alddasçorru; **(b)** Alddasçorru; **(c)** Nulpotjåkka, and; **(d)** Tarfalatjårro. For each sample three diffractograms are shown. In the bottom diffractograms the samples are untreated, in the middle diffractograms the samples are ethylglycolated, and in the top diffractograms the samples are heated to  $550^\circ\text{C}$ . These diffractograms illustrate the range of minerals present (labelled) in the Alddasçorru, Duopteçohkka, and Tarfalatjårro blockfields, and in the till samples. Poorly crystallized oxyhydroxides produce a rise in the diffractogram baseline, which disappears on heating, at d-spacings between 5 and  $3.5 \text{ \AA}$  (pink-filled circles). Vermiculization of chlorite and/or mica is shown by peaks in the  $\sim 10\text{--}14 \text{ \AA}$  (yellow) area that collapse to  $10 \text{ \AA}$  on heating. Gibbsite is shown by peaks at  $4.9 \text{ \AA}$  (green), which also collapse on heating.

**Arctic-alpine  
blockfields in  
northern Sweden**

B. W. Goodfellow et al.

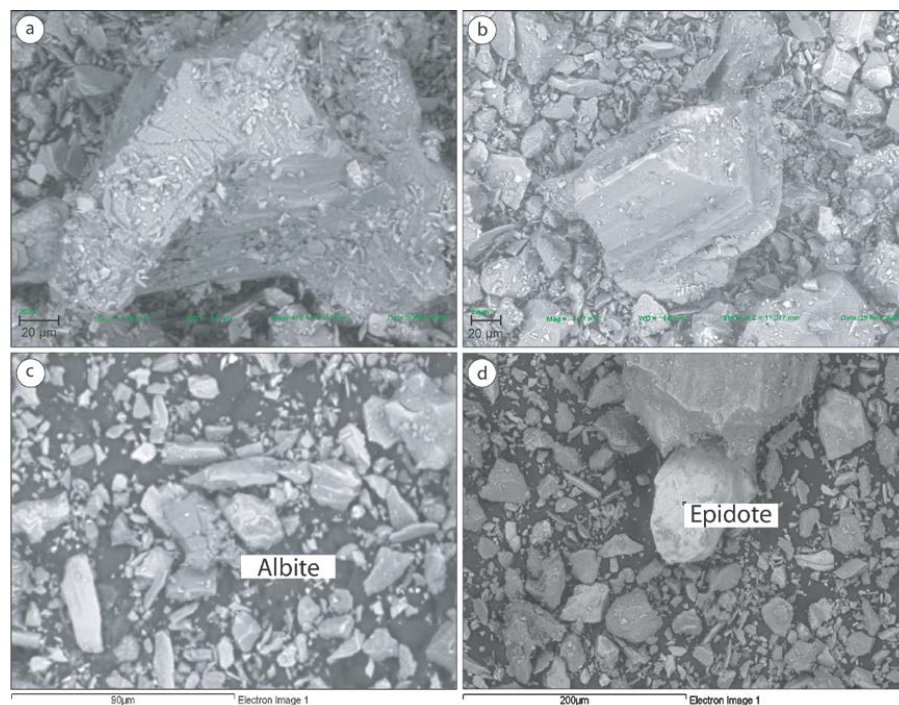


**Fig. 5.** SEM images indicating only slight chemical weathering of fine matrix. **(a)** Albite, with a chemically etched surface; the only etched grain identified (BG-05-84, Tarfalatjärro pit 7). **(b)** Chemically unaltered amphibole, typical of all SEM images of amphibole (BG-05-26, Aldasčorru pit 2). **(c)** Disintegrating albite, possibly through chemical processes (BG-05-11, Aldasčorru pit 1). **(d)** Chemically unaltered epidote, typical of all SEM images of epidote (BG-05-04, Aldasčorru pit 1).

Title Page

Abstract

Introduction

Conclusions

References

Tables

Figures

◀

▶

◀

▶

Back

Close

Full Screen / Esc

Printer-friendly Version

Interactive Discussion



## Arctic-alpine blockfields in northern Sweden

B. W. Goodfellow et al.

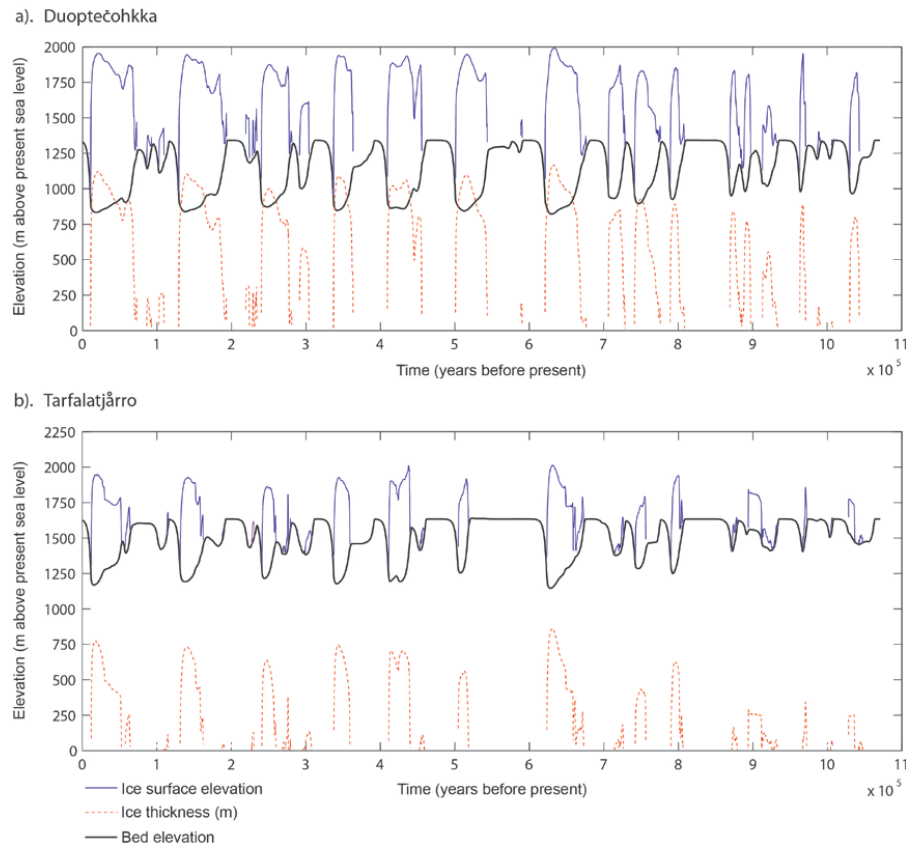


**Fig. 6.** Modelled ice sheet surface elevation, ice thickness, and bedrock response to ice sheet loading and unloading for **(a)** Duoptečohkka and **(b)** Tarfalatjärro over the last 1.07 Ma. These data were generated using a 3-dimensional ice-dynamical model forced by the Lisiecki and Raymo (2005) stack of global benthic  $\delta^{18}\text{O}$  records and the ELRA bedrock model (Bintanja et al., 2002, 2005).

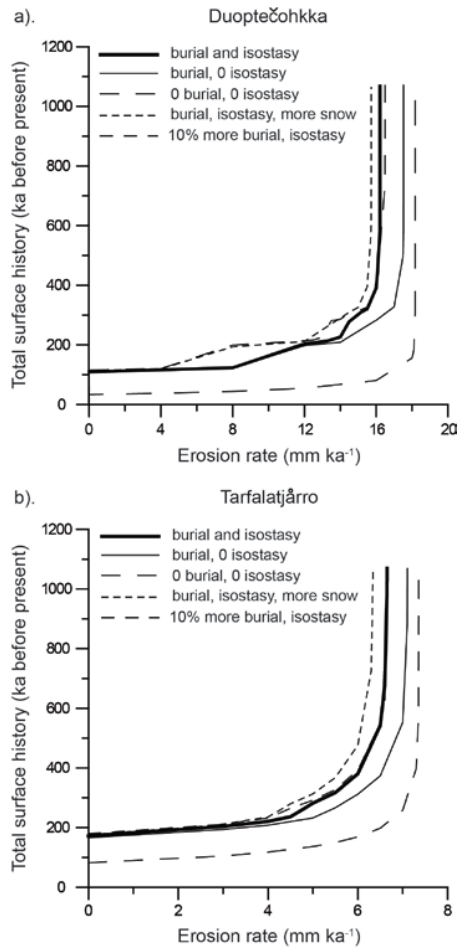


Fig. 7. Caption on next page

**Arctic-alpine  
blockfields in  
northern Sweden**

B. W. Goodfellow et al.

Title Page

Abstract Introduction

Conclusions References

Tables Figures

◀ ▶

◀ ▶

Back Close

Full Screen / Esc

Printer-friendly Version

Interactive Discussion



## Arctic-alpine blockfields in northern Sweden

B. W. Goodfellow et al.

**Fig. 7.** Total surface histories for **(a)** Duoptečohkka and **(b)** Tarfalatjårro plotted against surface erosion rates. These histories are modelled using  $^{10}\text{Be}$  concentrations in regolith surface quartz clasts and incorporate periods of burial by ice sheets and changes in  $^{10}\text{Be}$  production rates attributable to glacial isostasy through the use of a 3-dimensional ice-dynamical model (Bintanja et al., 2002, 2005). Seasonal burial of ground surfaces by 30 cm of snow for 7 months of the year is included. Steps in the total surface histories are caused by periods of ground surface burial by ice sheets. To explore the sensitivity of derived maximum erosion rates to these input parameters we modelled 5 different scenarios. The first scenario, as described above, includes the effects of ice sheet burial duration and glacial isostasy (marked “burial and isostasy” in the plots) and is our primary model output. In the second scenario (“burial, 0 isostasy”), isostasy is removed. In the third scenario (“0 burial, 0 isostasy”), a simple surface exposure history is modelled, from which burial and glacial isostasy are excluded. The fourth scenario (“burial, isostasy, more snow”) replicates the first scenario except that snow depth and snow cover duration are increased to 50 cm and 10 months of the year, respectively. In the fifth scenario (“10 % more burial, isostasy”), each burial period is extended by 10 % (and exposure periods commensurately shortened). The primary model scenario indicates maximum erosion rates of  $16.2\text{ mmka}^{-1}$  for Duoptečohkka and  $6.7\text{ mmka}^{-1}$  for Tarfalatjårro. The full ranges of maximum erosion rates are  $15.5\text{--}18.0\text{ mmka}^{-1}$  and  $6.0\text{--}7.3\text{ mmka}^{-1}$  for Duoptečohkka and Tarfalatjårro, respectively. Maximum total surface histories are infinite. However, despite acknowledged uncertainties in input values, all modelled total surface histories are confined to the late Quaternary before they become asymptotic.

Title Page

Abstract

Introduction

Conclusions

References

Tables

Figures

◀

▶

◀

▶

Back

Close

Full Screen / Esc

Printer-friendly Version

Interactive Discussion

